UNIVERSITAT POMPEU FABRA

DOCTORAL THESIS

Analysis of Brain Dynamics Using Echo-State Networks

Author:
David Ibáñez Soria

Supervisor:
Dr. Jordi García Ojalvo
Dr. Aureli Soria-Frisch

Caminante, son tus huellas
el camino, y nada más;
caminante, no hay camino,
se hace camino al andar.
Al andar se hace camino,
y al volver la vista atrás
se ve la senda que nunca
se ha de volver a pisar.
Caminante, no hay camino,
sino estelas en la mar.

Antonio Machado

UNIVERSITAT POMPEU FABRA

Abstract

Biomedical Engineering Program

Doctor of Philosophy

Analysis of Brain Dynamics Using Echo-State Networks

by David Ibáñez Soria

In the last decade recurrent neural networks have revolutionized the field of artificial intelligence. Their cyclic connections provide them with memory and thus with the capability of modeling processes with temporal context. Echo-state networks are a framework for recurrent neural networks that enormously simplifies their design and training. In this thesis we explore the capabilities of echo-state networks and their application in EEG feature extraction and classification problems. In a first study, we proved that such networks are capable of detecting generalized synchronization changes between two chaotic time-series. In a second study, we used echo-state networks to characterize the non-stationary nature of what has been considered so far to be a stationary brain response, namely steady-state visual evoked potentials (SSVEPs). Finally, in a third study, we successfully proposed a novel biomarker for attention deficit hyperactivity disorder (ADHD), which is capable of quantifying EEG dynamical changes between low and normal attention-arousal conditions. The results presented here demonstrate the excellent non-stationary detection capabilities of these networks, and their applicability to electrophysiological data analysis.

Resumen

En la última decada las redes neuronales recurrentes han revolucionado el campo de la inteligencia artificial. Sus conexiones cíclicas les proporcionan memoria y por tanto la capacidad de modelar problemas con contexto temporal. Las redes *echo-state* simplifican enormemente el diseño y entrenamiento de las redes recurrentes. En esta tesis exploramos el uso de redes *echo-state* y su aplicación en problemas de clasificación y detección de patrones en señales EEG. En un primer estudio demostramos que son capaces de detectar cambios de sincronización generalizada entre dos series temporales caóticas. En un segundo utilizamos redes *echo-state* para caracterizar la no estacionaridad de un fenómeno considerado de estado estable, potenciales visuales evocados steady-sate (SSVEP). Finalmente en un tercer estudio proponemos un nuevo biomarcardor para TDAH capaz de cuantificar cambios en la dinámica de la señal EEG entre condiciones bajas y normales de excitación. Los resultados aquí presentados demuestran la excelente capacidad de detección de patrones no estacionarios de estas redes, así como su aplicabilidad en el análisis de datos electrofisiológicos.

Resum

En l'última dècada les xarxes neuronals recurrents han revolucionat el camp de la intel·ligència artificial. Llurs connexions cícliques els proporcionen memòria i, per tant, la capacitat de modelar problemes amb context temporal. Les xarxes *echo-state* simplifiquen enormement el disseny i entrenament de les xarxes recurrents. En aquesta tesi explorem l'ús de xarxes *echo-state* i la seva aplicació en problemes de classificació i reconeixement de patrons en senyals d'EEG. En un primer estudi demostrem que són capaços de detectar canvis de sincronització generalitzada entre dues sèries temporals caòtiques. En un segon, emprem xarxes *echo-state* per caracteritzar la part no estacionària d'un fenomen considerat estable fins ara, els anomenats potencials visual evocats d'estat estable (SSVEP - acrònim en anglès). Finalment, en un tercer estudi, proposem un nou marcardor per al TDAH que permet quantificar els canvis en la dinàmica del senyal EEG entre condicions baixes i normals d'activació. Els resultats aquí presentats demostren l'excel·lent capacitat de detecció dels processos no estacionaris de les xarxes*echo-state* així com la seva aplicabilitat en l'anàlisi de dades electrofisiològiques.

Preface

The idea of doing a PhD started in 2008 while pursuing my master's thesis at Philips Research. It was there, and accidentally, that I first discovered computational neuroscience and scientific research. There was some magic in simply putting a wired cap on someone's head and starting to look at the electricity produced by their brain. The best part was to confront these dirty and noisy signals and extract information out of them. There was no manual, all that was needed was patience, hard work, a lot of reading and a bit of imagination. Six years later, and with other professional experiences in between, I finally decided to enroll the thesis work presented here.

When looking at a temporal EEG series, one immediately realizes that the brain is not steady-state, nor stationary. Nature is dynamic and so is the brain. The brain is chaos, complexity, coupling and decoupling, noise, synchronicity, fluctuations, and interactions. Stationary analysis of neural time-series, such as rhythmic band power monitoring, is still largely employed in computational neuroscience. However, the nature of the brain advocates for the use of non-stationary techniques capable of detecting richer signal dynamics.

Recurrent neural networks incorporate feedback connections or loops, which allows them to encode temporal information and converts them into a dynamical system. In this thesis I investigate the use of recurrent neural networks, in their echo-state form, for the dynamical characterization and classification of neural time-series. I hope with this work to have contributed my bit to the development of this field.

Acknowledgements

In the first place, I would like to thank my thesis directors. Aureli, Jordi, thank you very much for all the time spent with me during these four years, for the scientific discussions, the guidance, the paper reviews, and for understanding the special conditions in which I was carrying out this PhD. I also want to thank Starlab for giving me the opportunity and facilities to pursue this PhD. Special thanks to Giulio Ruffini for his advice and involvement.

A warm thanks to all my colleagues at Starlab Neuroscience who in one way or another have participated in this long story: Anton, Alejandro, Javier, Steve, Marta, Eleni, Andrés, thank you. Thanks to Mateu Servera and his team at the Universitat de les Illes Balears for their collaboration and counselling. Thank you to Gary García for his kind but rigorous initiation in the field of computational neuroscience and to Mieranda Vlot for the linguistic review of this manuscript.

I would also like to thank my family and friends who have accompanied me along the way, with special thanks to my parents for always being present and supportive. You have taught me the importance of persistence, hard work and not giving up just because things go sideways. My final and most important thanks goes to Elsa and Alba. Elsa, thank you for your kindness, support, understanding and patience in the good and especially in the bad moments. I know that without you by my side this PhD would not have been possible. And Alba... thank you for showing me the relative importance of all this compared to what really matters.

Contents

List of Figures

List of Tables

List of Abbreviations

ADHD	**A**ttention **D**eficit **H**yperactivity **D**isorder
ANN	**A**rtificial **N**eural **N**etworks
AS	**A**lmost **S**ynchronization
ASD	**A**utism **S**pectrum **D**isorder
AT	**A**ssistive **T**echnology
BCI	**B**rain **C**omputer **I**nterface
BPTT	**B**ack **P**ropagation **T**hrough **T**ime
CCA	**C**anonical **C**orrelation **A**nalysis
CFC	**C**ross-**F**requency **C**oupling
CPT	**C**ontinuous **P**erformance **T**ask
CS	**C**omplete **S**ynchronization
DC	**D**irect **C**urrent
DPLS	**D**ouble-**P**artial **L**east-**S**quares
DR	**D**ynamical **R**eservoir
DSM	**D**iagnostic and **S**tatistical **M**anual of Mental Disorders
EEG	**E**lectro **E**ncephalo**G**raphy
EOG	**E**lectro **O**culo**G**raphy
ERP	**E**vent-**R**elated **P**otential
ESN	**E**cho-**S**tate **N**etworks
ESP	**E**cho-**S**tate **P**roperty
EU	**E**uropean **U**nion
FDA	**F**ood and **D**rug **A**dministration
FFT	**F**ast **F**ourier **T**ransform
FT	**F**ourier **T**ransform
FMRI	**F**unctional **M**agnetic **R**esonance **I**maging
GC	**G**ranger **C**ausality
GS	**G**eneralized **S**ynchronization
ICA	**I**ndependent **C**omponent **A**nalysis
ICD	**I**nternational Statistical **C**lassification of **D**iseases

IPC	**I**ntersite **P**hase **C**lustering
ITR	**I**nformation **T**ransfer **R**ate
LASSO	**L**east **A**bsolute **S**hrinkage and **S**election **O**perator
LFP	**L**ocal **F**ield **P**otentials
LS	**L**ag **S**ynchronization
LSTM	**L**ong **S**hort **T**erm **M**emory
LZW	**L**empel **Z**iv **W**elch
MEG	**M**agneto **E**ncephalo**G**raphy
MLP	**M**ulti**L**ayer **P**erceptron
MSC	**M**agnitude-**S**quared **C**oherence
MSI	**M**ultivariate **S**ynchronization **I**ndex
NIRS	**N**ear **I**nfra-**R**ed **S**pectroscopy
PAF	**P**eak **A**lpha **F**requency
PAC	**P**hase-**A**mplitude **C**oupling
PCA	**P**rincipal **C**omponent **A**nalysis
PDF	**P**robability **D**ensity **F**unction
PET	**P**ositron **E**mission **T**omography
PPC	**P**hase-**P**hase **C**oupling
PS	**P**hase **S**ynchronization
PSD	**P**ower **S**pectral **D**ensity
PSDA	**P**ower **S**pectral **D**ensity **A**nalysis
RC	**R**eservoir **C**omputing
RNN	**R**ecurrent **N**eural **N**etworks
RVS	**R**epetitive **V**isual **S**timulation
SL	**S**ynchronization **L**ikelihood
SNR	**S**ignal to **N**oise **R**atio
SSVEP	**S**teady **S**tate **V**isual **E**voked **P**otential
TBPTT	**T**runcated **B**ack **P**ropagation **T**hrough **T**ime
TBR	**T**heta **B**eta **R**atio
TDAH	**T**rastorno de **D**éficit de **A**tención e **H**iperactividad
USA	**U**nited **S**tates of **A**merica
WT	**W**avelet **T**ransform

To Alba

1 Introduction

1.1 Motivation and General Goals

We are currently witnessing the machine and deep learning revolution. The artificial intelligence era has brought us face and speech recognition, self-driving cars, conversations with Siri, Alexa and Cortana, and online search algorithms that have changed the way we interact with the world. It has already transformed fields such as healthcare, economics, marketing, security and communication. Its success comes from the fact that machine learning algorithms do not need to be explicitly programmed, they are fed with data and automatically adapt their parameters, based on the information provided. One of the most popular machine learning models are neural networks. They are biologically inspired by brain function and consist of a finite network of interconnected artificial neurons. Neural networks are not new, in the late 1950s MADALINE was the first neural network applied to a real-world problem [1], however, their use remained limited for decades. A renaissance started in 1980s with the application of the backpropagation algorithm to neural networks training [2]. Recent advances in computer processing capabilities and parallelization, network architectures, learning algorithms and data availability have unleashed their potential and led to their widespread use. A particularly interesting application of neural networks is in the understanding of the brain itself [3][4].

The brain is a dynamic system that produces nonlinear electrical activity [5] that can be measured through electroencephalography (EEG), among other brain monitoring techniques. Methodologies capable of detecting neural complexity, temporal dynamics and synchronicity between brain sources are therefore necessary for the analysis and understanding of brain functioning. Recurrent neural networks (RNN) are a neural network family that is characterized by incorporating cyclic connections which provide

memory and the capability of decoding non-stationary temporal information.

Many architectures for the construction and training of RNNs exist, while the one adopted in this Thesis is Reservoir Computing (RC) in its Echo-State Network (ESN) modality [6]. ESNs appeared as a new approach towards understanding and training recurrent neural networks based on the principle that if the network fulfills certain properties, adaptation of all connections between neurons is not necessary to solve prediction problems. During the training, therefore, most connections are randomly generated. This property is known as the Echo-State Property (ESP) and is accomplished if the dependency to initial conditions is lost with time [6]. ESNs thus enormously simplify the training process and reduce its computational cost with respect to other RNNs architectures. Echo-state networks have proved to deliver excellent performance in many tasks and applications in economics, physical modeling, optics and robotics. They are currently an active research topic [7][8] and a valuable approach in physiological characterization [9].

Stationary methodologies are widely used in EEG characterization. Approaches such as spectral analysis still hold as state-of-the-art in many fields. The general objective of this Thesis is to investigate brain dynamics by using echo-state networks in the analysis of electrophysiological data. We aim to develop efficient methods capable of characterizing neural non-stationary dynamics and compare their performance with existing stationary approaches. In this first chapter we intend to introduce every specific topic addressed in this Thesis, with the objective of providing the necessary background for a good understanding of the following chapters.

1.2 Chaotic Dynamics and Synchronization

The study of brain dynamics aims at mathematically characterizing neural activity in order to understand the underlying brain process and its correlation with physical and mental states. This study can be approached following different strategies. Conventional approaches are based on linear models which study neural stationary dynamics.

The brain produces complex, nonlinear dynamics that can be measured through the EEG [10]. In particular, EEG signals have also been considered to be the result of nonlinear dynamic systems that exhibit chaotic behavior [11]. Since the mid-1980s chaos theory has been applied to the analysis of neural dynamics with increased interest from the scientific community [12][13]. This chaotic behavior is considered to "serve as the essential ground state for the neural perceptual apparatus" [14]. The brain has been observed to behave as a deterministic chaotic attractor, for example, during epileptic seizures [11]. In this Thesis we follow this latter approach to characterize and study the brain dynamics as a nonlinear phenomenon. Therefore, we have adopted a machine learning approach in the form of echo-state networks (ESNs), which is capable of capturing nonlinear dynamics and the chaotic nature of brain signals [15].

In this Thesis we attempt to analyze the relationships between structural and functional brain sources as a chaotic synchronization problem. To validate the capabilities of ESNs in the detection of chaotic synchronization (in its generalized synchronization form), we have conducted a theoretical work, which is presented in Chapter 2, which proves their capability of accurately detecting changes in generalized synchronization between two coupled attractors. When ESNs are applied in the analysis of neural time-series, they are used in a fashion so that they are capable of detecting dynamic patterns, but also complex relationships between EEG channels. These works are presented in Chapters 3 and 4. In this section we introduce the differences between stationary and non-stationary systems. Subsequently we introduce chaotic systems, how they can be synchronized, and the most relevant forms of synchronization between chaotic systems.

1.2.1 Stationary and Non-Stationary Systems

Digital signal processing (DSP) studies time-series digitally collected. This process implies the discretization of the amplitude of continuous temporal observations that are mapped into a finite set of values [16]. Mathematically, these time series can be seen as stochastic processes that can be divided into stationary and non-stationary [17]. Stationary processes are characterized by statistical properties that are invariant over time, and are therefore easily predictable. Standard deviation, covariance and mean are

examples of time-invariant statistical metrics that can be used to characterize stationary signals.

Formally speaking, a stationary stochastic process is strictly or strongly stationary if its joint probability distribution does not change when shifted in time [18]. Joint distributions quantify the relationship between two or more events, while the probability density function (PDF) describes the relative likelihood for a random variable to take on a given value. As a consequence, all moments of a stationary process are the same no matter the instant at which they are measured. Purely random distributions such as the Gaussian distribution are examples of stationary processes. The probability density function of a Gaussian distribution, for example, is only characterized by its mean or expectation (μ) and its variance (σ^2).

Real-world data evidences that strong stationarity and purely Gaussian processes are distributions rarely found [19]. The definition of strong stationarity is thus too strict for most processes and a less rigid approach is needed for real-world observations. The definition of weak stationarity only concerns the shift-invariance of first and second moments of a process. In non-stationary processes statistical properties such as the mean, variance and covariance change over time. Non-stationary signals thus show trends, events, and cycles that make it difficult (or in many cases impossible) to be forecasted or modeled.

1.2.2 Chaotic Systems

Non-stationary systems are dynamical processes whose internal state variables follow temporal rules [20]. They consist of a state space whose coordinates describe the state at a given time and a dynamical rule that drives the immediate future state based on current ones. There are two main types of dynamical system, with discrete and continuous time. Continuous time dynamical systems are expressed using ordinary, partial or delayed differential equations (ODEs, PDEs, DDEs), while in discrete systems, the states update in time is defined as a mapping.

Chaotic systems are dynamical systems that show high sensitivity to initial conditions. Many examples of chaotic systems exist, among them the

Rössler attractor. This system, defined by the following nonlinear ODE, and whose trajectories are displayed in Figure 1.1, has been employed in Chapter 2.

$$dx/dt = -y - z$$
$$dy/dt = x + ay$$
$$dz/dt = b + z(x - c)$$

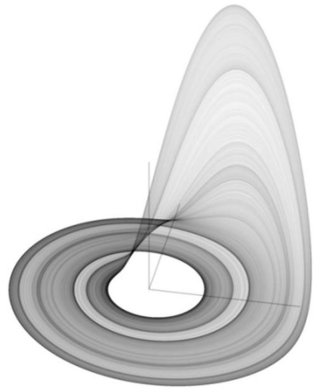

FIGURE 1.1: The Rössler attractor in its chaotic mode (Figure taken from [21]).

1.2.3 Synchronization in Chaotic Systems

Due to their long-term unpredictable nature, chaotic systems seem to defy synchronization. Two identical chaotic systems starting from slightly different initial conditions will show trajectories that would exponentially separate. Therefore the term synchronization shall be re-defined when referred to chaotic systems. Synchronization occurs when chaotic systems are coupled in a way that they adjust their trajectories. It has been defined by Boccaletti as "the process wherein two (or many) chaotic systems (either equivalent or nonequivalent) adjust a given property of their motion to a common behavior, due to coupling or forcing. This ranges from complete agreement of trajectories to locking of phases [22]".

There are two possible configurations to achieve synchronization between

two chaotic systems: unidirectional and bidirectional coupling. Unidirectional coupling can be achieved in master–slave configuration, where one system freely evolves and drives the evolution of the other. In bidirectional coupling both systems influence the evolution of each other, inducing an adjustment of the trajectories onto a common manifold. Different synchronization states can be produced between chaotic systems, among them: complete synchronization (CS) [23], phase synchronization (PS) [24], lag synchronization (LS) [25], almost synchronization (AS) [26] and generalized synchronization (GS) [27]. As explained in Chapter 2, in this Thesis two Rössler attractors have been synchronized via unidirectional coupling in order to produce time sequences that exhibit generalized synchronization.

The generalized synchronization phenomenon describes a non-trivial synchronization between the trajectories of two non-identical coupled systems. As it will be further explained in Chapter 2, one example of how to achieve generalized synchronization between two different coupled attractors was proposed by Rulkov in [27]. Taking two different attractors X and Y, with completely synchronized trajectories as displayed in Figure 1.2A, Rulkov proposed to apply a nonlinear transformation to Y converting it into Z. Figure 1.2B shows the relationship between X and Z, where a straight line denoting identical synchronization is no longer observed, but a complex relationship between the attractors exists. In spite of this lack of linear correlation, synchronization has not been lost since only a nonlinear transformation was applied to completely synchronized systems. In this case it can be determined that both systems show generalized synchronization. Several methodologies for the detection of generalized synchronization exist, including the replica method, the synchronization likelihood, and the mutual false nearest neighbor method [28][29]. In Chapter 2 we propose an alternative methodology based on echo-state networks.

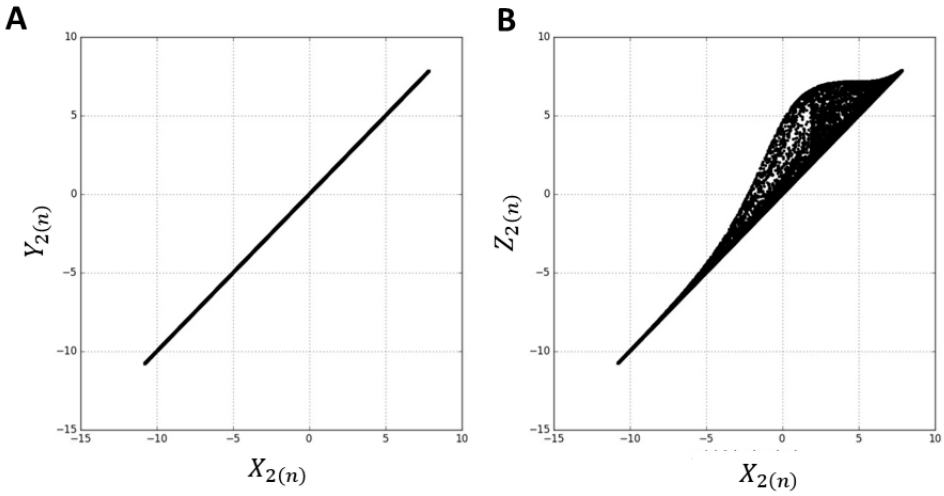

FIGURE 1.2: A) Identical Synchronization between $X_2(t)$ and $Y_2(t)$, B) Generalized Synchronization between $X_2(t)$ and $Z_2(t)$

1.3 Echo-State Networks

Machine learning is a subfield of computer science and artificial intelligence that aims to build computer systems that automatically adapt their parameters in order to make accurate predictions based on experience [30]. This experience is given in the form of data observations or examples.

Supervised machine learning, the approach used in this Thesis, uses labeled examples to predict a system output. In practice, using a training signal consisting of a set of data observations and their target output (denoted herein as teacher-forced-output), the machine learning algorithm adapts the values of its variables to make predictions. The trained machine learning algorithm can thus be used for mapping unseen examples. These algorithms are usually self-adapted through the minimization of what is known as its cost function, generally a function of the error between the target and the output. The cost function also provides a metric on how well the algorithm learned the regression or classification problem for which it was trained.

A popular supervised machine learning approach are artificial neural networks (ANN). ANNs have stirred up the field of artificial intelligence due to their excellent information processing capabilities. They have proved capable of accurately modeling complex real-world problems due to their noise tolerance, high parallelism, capability to generalize and the fulfillment of the representation theorem [31][32]. In this Thesis we investigate the capabilities and applicability to electrophysiological analysis of Echo State Networks (ESNs). For this reason, in this section we first introduce ANNs taking as starting point their most simple form, the artificial neuron. We later provide a detailed explanation of ESNs capabilities, architecture, parameterization and training.

1.3.1 Artificial Neurons

Ramón y Cajal, considered by many as the father of modern neuroscience, first introduced the idea that individual cells, later called neurons [33], were the structural constituents of the human brain. Cajal demonstrated that the nervous system was formed by a network of millions of interconnected neurons capable of transmitting information. Figure 1.3 shows one of Cajal's depictions of a neural ensemble. The mechanism by which neurons communicate with one another is known as synaptic coupling [34].

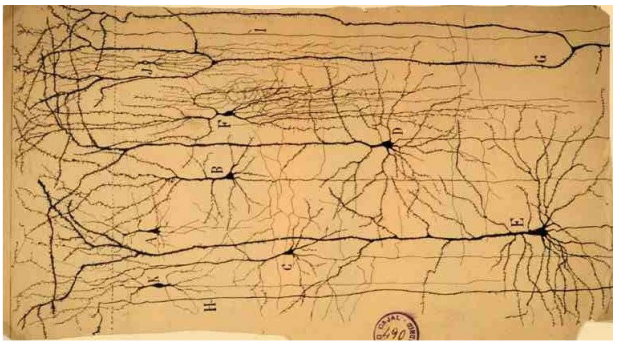

FIGURE 1.3: Santiago Ramón y Cajal (1899), Human Brain Cortex

During the synaptic transmission process, the post-synaptic neuron receives in its dendrites electrochemical spikes, which can be either excitatory or inhibitory. A single neuron can receive thousands of synaptic inputs from many different pre-synaptic neurons. The post-synaptic neuron integrates these inputs, and depending on the outcome of the integration, the neuron can fire transmitting its action potential to other neurons connected to its axon. The human cortex is estimated to contain approximately 10 billion neurons and 60 trillion synaptic connections [35].

Artificial neural networks (ANNs) are biologically-inspired information processing implementations that imitate the functioning of the brain. The basic information-processing unit of ANNs is called neuron, but also referred to as node or unit. Frank Rosenblatt's perceptron [36] is considered the first artificial neural network. It consists of a single layer network that works as a linear binary classification predictor. Artificial neurons integrate input signals through connecting links that model synaptic connections. These links are characterized by a fixed weight or strength which is set during the training process. Figure 1.4A displays a graphical representation of an artificial neuron with n connecting links. The signals x_i feed the neuron multiplied by its corresponding weight w_i. Weighted inputs are then linearly combined in the summing junction. It is important to remark that synaptic weight ranges include negative and positive values, and can therefore act as inhibitory or excitatory links. A bias factor is then applied for lowering or increasing the input of the activation function. The activation function transforms the weighted averaged inputs into an output value y that is transmitted to other connected neurons. Activation functions can be linear and nonlinear. Among most used activation functions are the step, identity, hyperbolic tangent, sigmoid or rectified linear unit.

1.3.2 Artificial Neural Networks

Rosenblatt's perceptron is only capable of solving linearly separable problems, a factor that remarkably limits its applicability to real-world problems. A solution to overcome this limitation is to use layers of interconnected neurons constructing what is known as a multilayer perceptron (MLP) [37]. MLPs are organized in three layers of neurons: input, hidden and output. Figure 1.4B depicts the MLP architecture. Input weights

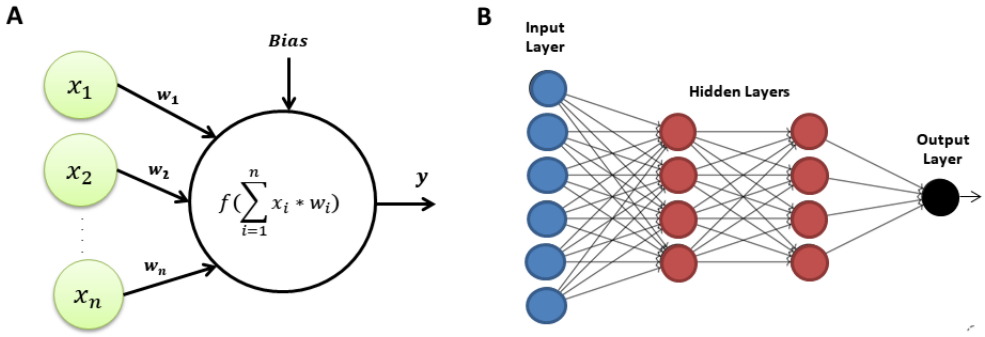

FIGURE 1.4: A) Artificial neuron diagram B) Multilayer perceptron with two hidden layers

(W_{in}) connect the input nodes into the hidden layer. Internal weights (W) connect nodes between hidden layers among them. Finally output weights (W_{out}) map the hidden nodes into output nodes. During the training process, input, hidden and output connection weights are optimized in order to minimize the error between the network and the desired teacher output. The development of back-propagation algorithms in the mid-1980s revolutionized neural networks, providing a computationally efficient method for training MLPs [38]. Static neural networks such as the MLPs are implemented in a feed-forward fashion, with information flowing from input to output. Feed-forward systems thus treat each example one by one, being incapable of retaining states and thus of detecting temporal context.

Adding feedback connections allows an MLP to encode information with temporal context and thus to incorporate memory, converting it into a dynamical system. There are two basic approaches of incorporating feedback: local feedback, which is applied to a single neuron, and global feedback, which is implemented as recurrent connections within and/or among neurons of different layers [39]. Recurrent networks have recently gone from impractical to being a widely used approach thanks to recent advances in architectures, training algorithms, and parallel computing [40]. The main issue in recurrent neural networks, as in all nonlinear dynamical systems, is their potential instability as explained in the literature [41]. With conventional descending gradient-based algorithms such as back propagation

through time (BPTT), error signals propagating backwards in time tend to either blow up or vanish [42]. Truncated backpropagation through time (TBPTT) offers a solution to this problem [43]. In TBPTT a maximum number of time-steps in which the error is backwards propagated is constrained. Obviously, while a small number of time-steps solves the exploding vanishing gradient issue, it limits the network capability of detecting long-time dependencies. Modern neural networks such as long-short term memory (LSTM) architectures [44] overcome this limitation.

1.3.3 Echo-State Networks

In 2001 a new approach for recurrent neural networks was proposed independently and simultaneously by Jaeger under the name of Echo State-Networks (ESN) [6], and Maass under the name of Liquid State Machines (LSM) [45]. Both together constituted a new trend towards understanding, training, designing and applying RNNs, grouped under what came to be known as Reservoir Computing (RC) [46]. Today, RC has incorporated other related methods and extensions developed since, such as Backpropagation-Decorrelation [47] and Evolino [48].

Figure 1.5 shows a basic ESN architecture. The depicted network has two input units ($N_i = 2$), a single output unit ($N_o = 1$) and five internal or hidden units ($N = 5$). Input, internal, back-propagation and output connectivity weights are respectively represented by W^{in}, W, W^{back} and W^{out}. ESNs without output to hidden layer back-propagation connections, as the one presented here, are the typical choice for purely input-driven pattern recognition and classification tasks. This is the architecture that has been applied in this Thesis. The two-dimensional signal $u(n)$ of N_s timing-points inputs the network that produces the output signal $y(n)$.

ESNs are based on the principle that if the network fulfills what is known as the echo-state property (ESP), then the adaptation of all weights is not necessary, and therefore most of the network connections can be randomly generated [49]. The echo-state property is satisfied if the state of the network asymptotically depends only on the input signal, implying that initial condition dependencies are progressively lost. In practice, input and back-propagation weights do not affect the echo-state property, which only

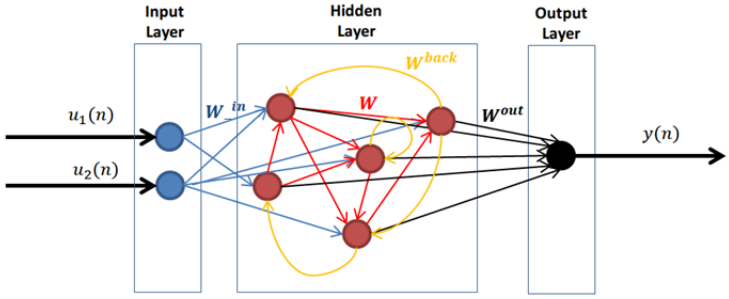

FIGURE 1.5: Echo-state network architecture with two input, five hidden and one output unit.

depends on internal weights. It has been noticed that the ESP is granted if the spectral radius, calculated as the largest absolute eigenvalue of hidden connections, is smaller than the unity [50]. This fact has led to an erroneous identification of the ESP with a spectral radius smaller than one. It has been demonstrated that the ESP depends on the nature of the input signal and the algebraical characteristics of the dynamical reservoir [51][52]. In general, the larger the input, the further above unity the spectral radius can be while the ESP still holds. Therefore, there is not yet a theoretical principle whereby the spectral radius can be set a priori, being necessary its ad-hoc adaptation.

The Dynamical Reservoir

The untrained network with randomly generated weights forms the dynamical reservoir (DR) and consists of input, back-projection and internal weights. The ESN approach enormously simplifies RNNs, providing a computationally inexpensive method in which adaptation of all weights is not necessary, but only readout connections need to be trained.

ESNs are not yet a perfectly mature approach and further advances, extensions and demonstrations of their practical applicability shall be addressed. One important line of research is currently the reservoir construction. Random creation of the dynamical reservoir delivers excellent classification and accuracy results in many tasks, however the effects of the network topology on task performance in many cases remain uncertain. Advances in the understanding of the reservoir characteristics effects may lead to a more optimal and efficient reservoir design. Several reservoir optimization algorithms are currently being investigated, which according to Lukosevicius [53] can be grouped in 1) generic, 2) unsupervised pre-training in which the reservoir is pre-trained with respect to the input, and 3) supervised pre-trained in which the reservoir is constructed based on the input and target data. In this Thesis work we do not investigate the reservoir topology and its implications in the network dynamics, following instead the generic method. This method is considered the classic form of constructing DRs and is the most used. It has proven to deliver good results irrespective of input and target adaptation.

To construct an appropriate reservoir following the generic method [53], the hidden layer shall be large, sparse, and random. The rationale is that many internal units guarantee rich dynamics, sparse connectivity loosely couples activation signals, and random connections guarantee different dynamics. The reservoir is generally constructed using a symmetric distribution of connecting weights around the zero values. Input and back-propagation weights are usually dense (although they can also be sparse) and generated using a uniform distribution. Echo-state networks standardly use sigmoid activation functions.

The DR provides temporal context and works as a nonlinear expansion of the input. The idea behind ESNs is that random connections in the reservoir allow known states to echo. If the reservoir receives an input with states similar to those which it was trained on, its dynamics will start following these known trajectories. Therefore the reservoir should provide rich dynamics that are extracted as a linear combination of the output weights [54]. In general, the number of units in ESNs is larger compared to other machine learning approaches. Reservoirs of thousands of neurons are not uncommon, as we will see in the following chapters. The larger the

reservoir is the richer its dynamics, although it is important to be aware of the possible over-fitting if a large number of internal units is chosen, which would lead to poor generalization [55].

ESN Training

In ESN training, the first step is to construct the dynamical reservoir, consisting of randomly generated input, internal and back-propagation weights. ESNs training is a supervised machine learning problem in which for a given training input (u_{train}) and target output (y_{target}), output weights (W^{out}) are learned to minimize the error between the network output and the desired target. The training input is passed through randomly generated input, internal and back-propagation connectivity matrices in order to obtain the N-dimensional signal X. ESN output (y) can therefore be expressed as $y = X * w^{out}$.

Output weights can be calculated using any linear regression or classification algorithm. Ridge regression, also known as Tikhonov regularization, is in general the most common approach to train ESNs [56]. In any case many other methods such as linear least-mean-square error or support vector machines have successfully been employed in ESNs training.

In ridge regression, additional information apart from the error between the output and desired target is introduced to the minimization problem. In ESNs, large readout weights can be very sensitive to deviations from training conditions leading to poor generalization and unstable solutions [57]. To overcome this problem, the cost function to be minimized in ESN training is the root-mean squared error between teacher-forced and ESN output plus the weighted magnitude of the squared output weights. The selection of the optimal regularization parameter λ, is in general assessed through extensive search on a logarithmic grid. The ESN ridge regression cost function can be depicted mathematically as:

$$Cost = \sum_{i=1}^{N_s} (y(s) - y_{target}(s)) + \lambda ||w^{out}||^2$$

Parameterization of Echo-State Networks

In this Thesis work we have followed the indications for applying ESN proposed by Lukosevicius [58]. In analogy to other machine learning approaches, the global parameters of ESNs rule its behavior and pattern-recognition capabilities. Their ad-hoc adaptation is crucial to achieve an optimal performance. Key global parameters in ESN training are the size of the hidden layer, the sparsity, the spectral radius, the leaking rate, and the input scaling. These factors are described in detail in what follows.

The Reservoir Size is crucial to construct reservoirs with rich dynamics, and is given by the number of internal units. For difficult tasks the reservoir should be as big as computationally affordable.

The Input Scaling drives the non-linearity of the reservoir. A general practice in ESNs is to scale together all inputs to a common scaling factor. Assuming the use of sigmoid activation functions, if input values are close to 0, input layer neurons operate virtually linearly. With large input values, neurons saturate and start acting as binary switches. Linear tasks thus require small input scaling factors while complex tasks demand larger ones.

The Spectral Radius is computed as the largest absolute eigenvalue of connectivity matrix of the hidden layer. This quantity governs the time-scale of the reservoir and determines how the influence of inputs remains in the system [54]. In general, long memory tasks require a larger spectral radius. On the other hand, a larger spectral radius has the effect of driving input signals into a more nonlinear region. Thus this quantity also has an influence on the DR dynamics.

The Sparsity determines the connectivity degree of the network. Although early ESN reports suggest to have a sparse reservoir, in practice sparse connections tend to give only a slightly better performance [58]. In large reservoirs however, sparsity can reduce computational costs during training.

The Leaking Rate determines the speed at which the reservoir updates the dynamics in case leaky-integrated discrete-time continuous-value artificial neurons are employed.

In summary, when selecting the ESN global parameters, one has to consider that the nonlinearity of the network is given by the scaling of input and internal weights (input scaling and spectral radius). The dynamics update speed is given by the leaking rate, if leaky-integrated neurons are employed.

ESN Training Summary

In summary, ESN construction and training can follow this recipe [50]:

1. Set a meaningful training input U and its corresponding teacher-forced output Y_{target}.
2. Select the reservoir global parameters: neuron activation, spectral radius, function, sparsity and reservoir size.
3. Create a random dynamical reservoir with the selected global parameters (w, w_{back}). Attach input units by creating random all-to-all connections (w_{in}).
4. Standardize input training data to zero-mean standard deviation one.
5. Multiply the input training data by the selected input scaling factor.
6. Pass the training data through the dynamical reservoir.
7. Discard the N initial transient samples.
8. Train the output weights using the selected linear regression methodology minimizing the error between the output and teacher-forced output.
9. The ESN is ready to use. Ensure that it generalizes well and that the performance is adequate feeding the system with unseen data. If the results are not satisfactory, further selection of global parameters may be necessary.

1.4 Electroencephalography

The brain produces non-stationary electrical activity which can be measured by electroencephalography (EEG). In this Thesis we study the application of echo-state networks to EEG feature extraction and classification problems. Because of this, in this section we introduce this technique, comparing it with other brain monitoring methods. We also describe the brain dynamics and rhythms that can be measured by the EEG, and show how EEG recordings are analyzed. We end up with a summary of the most relevant EEG feature extraction methodologies.

Two types of EEG techniques exist: intracranial and extracranial [59]. Intracranial EEG, also referred to as electrocorticography, records directly from the brain through surgically implanted electrodes pointing to specific brain areas. In contrast, extracranial EEG is a non-invasive technique that places the electrodes on the surface of the scalp. Scalp electrodes measure the voltage difference between the recording electrode and a reference electrode. Figure 1.6 shows Enobio®, a new generation non-invasive EEG device. In this Thesis we are focused exclusively on the analysis of extracranial EEG, and thus hereinafter any explicit mention to EEG refers to this technique [60].

FIGURE 1.6: Neuroelectrics Enobio® EEG sensor

EEG measures the pooled electrical activity generated by large numbers of neurons. When a broad population of neurons fire in a synchronized way and are spatially organized, their activity lines up creating waves that can reach the scalp [61]. From its early days, EEG has been characterized by its oscillatory activity. The first discoveries from Berger already mentioned rhythmic electrical activity recorded from the human scalp. This finding was followed by a popularization of Hebb's theory [62] stating that neurons do not work in isolation but rather tend to work in synchrony. The brain needs to integrate these widespread neural assemblies to carry out coordinated actions and thus synchronize them. Coordinated assemblies that produce coherent activity generate oscillations that can be seen in the EEG.

Neurons are interconnected and present feedforward and feedback loops that make it easier for them to fire collectively. The signal generated by the cooperative action of nearby neurons is known as local field potential (LFP). LFPs reflect the average behavior of the action potentials of large numbers of interacting neurons and are considered the building blocks of EEG [63]. To reach the scalp these electrical signals go through layers of tissue, fluids, the skull and the skin. All these layers have different electrical and conductivity properties distorting and attenuating the signal that is measured in the EEG. This process that takes place as LFPs are transferred to the scalp results in some loss of specific information [64]. Pyramidal cortical neurons mainly contribute to scalp voltage as they are well-aligned and fire in a synchronized manner. It has been estimated that about 50,000 of these neurons in the superficial cortical layers dominate the EEG signal [64]. Deep brain sources are difficult to measure in the EEG as neurons in subcortical structures are usually not as well spatially organized and also are further from recording electrodes [64]. Figure 1.7 shows a 32-channel, one-minute EEG recording to illustrate the type of signals that we will be analyzing.

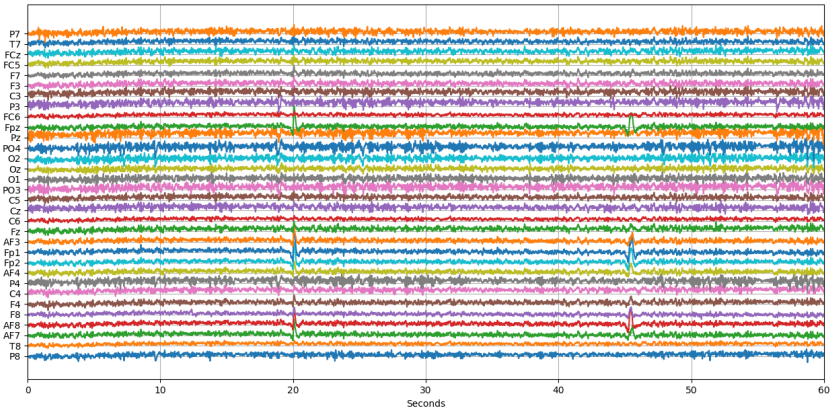

FIGURE 1.7: One-minute 32-Channel Electroencephalographic signal.

Besides EEG other brain monitoring methods exist, among them magnetoencephalography (MEG), functional magnetic resonance imaging (fMRI), positron emission tomography (PET) and near-infrared spectroscopy (NIRS). Figure 1.8 compares different brain monitoring techniques in terms of temporal resolution, spatial resolution, and of the degree of immobility necessary to perform good quality recordings. Compared to these techniques, EEG has poor spatial resolution, poor signal to noise ratio and low sensitivity to neural activity occurring below the cortex. On the other hand, EEG is significantly cheaper, customizable, and has an excellent temporal resolution (being able to achieve the order of micro-seconds). Additionally, the new generation of portable EEG devices such as Enobio, displayed in Figure 1.6, makes it possible to perform recordings outside laboratory conditions boosting the experimental possibilities. Besides, participants wearing wireless EEG devices can move during EEG assessments [65]. It is for all these reasons that EEG is a widely used brain monitoring technique in neuroscience.

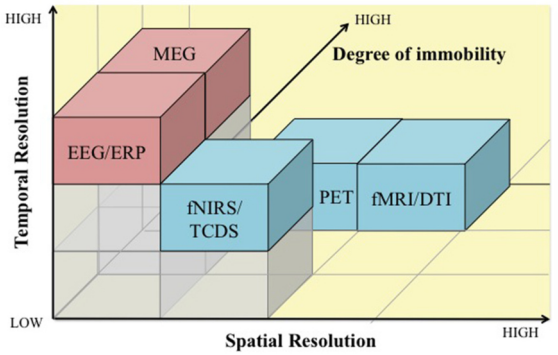

FIGURE 1.8: A comparison of brain monitoring techniques in terms of temporal resolution, spatial resolution, and degree of immobility (Figure taken from [65])

1.4.1 Brain Rhythms

Rhythmic EEG activity is grouped in bands, which are labeled with Greek letters following Berger [66]. Many definitions of EEG bands exist, a classification used commonly can be the following: Delta (δ): 0-4 Hz, Theta (θ): 4-8 Hz, Alpha (α): 8-12 Hz Beta (β): 12-30 Hz, and Gamma (γ) above 30 Hz. Rhythmic activity within a certain band has been seen to have a characteristic power distribution and to correlate with different physiological or cognitive functions. Below we summarize the traditional classification of EEG bands and their most relevant activity interpretation [67]–[69].

Delta: Irregular delta complexes in temporal regions appear in the healthy elderly population. Delta enhancement is linked to drowsiness onset and is seen during slow-wave sleep. It has also been linked to demanding sustained attention tasks. Abnormalities in the delta band are related to encephalopathies and usually indicate a structural lesion involving the white matter of the ipsilateral hemisphere.

Theta: Frontal theta activity is induced by emotions and sustained concentration. Theta activity is enhanced by hyperventilation, drowsiness and sleep. It is also linked to memory and emotion regulation.

Alpha: Alpha activity is enhanced by eye closing and is characterized by a dominant frequency within the alpha range known as individual

peak-alpha frequency (PAF). The alpha band is related to relaxation, aging, visual perception and attention.

Beta: Beta activity is enhanced during drowsiness, light sleep, anxiety, and with mental activation. Abnormal beta activity suggests cortical gray matter anomalies and drug effects.

Gamma: Gamma rhythms are related to perception, higher mental activity and consciousness.

As of today there is no agreement in standard frequency ranges and band distributions are often considered arbitrary "like the straight-line country borders between the African nations drawn by the colonialists" [60]. Some scientists have also expressed their skepticism about the value of brain oscillation research in advancing the understanding of brain processes underlying cognitive functions [70]. Figure 1.9 shows a typical EEG spectrum along with band power limits.

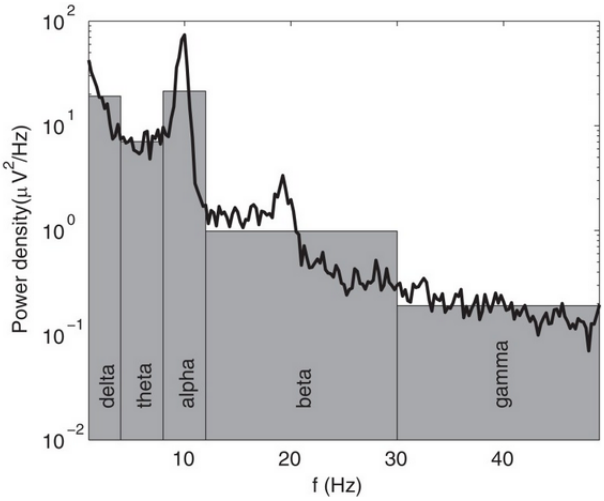

FIGURE 1.9: Example of an EEG spectrum (black line) with its approximation of band powers given by the areas of the gray bars (Figure taken from [71]).

1.4.2 EEG Preprocessing

The first step in EEG analysis is preprocessing. This stage aims at cleaning and preparing the data reliably for the subsequent feature extraction and classification phases. It is crucial to highlight the importance of working with reliable data. It does not matter which algorithms we use to decontaminate poorly recorded data, if the data quality is not sufficient for the analysis to be performed. It is thus a good practice when analyzing EEG series to discard those sequences where data-acquisition problems were reported or poor overall quality is detected.

A standard preprocessing pipeline cannot be defined as it has to be fully adapted to the experimental data and subsequent phases of the analysis, although some proposals have been done for enabling its automation [72]. Typical EEG preprocessing stages include: filtering, referencing, epoching, signal decomposition, artifact correction and artifact rejection, among others.

Filtering: The purpose of filtering is to remove unwanted frequency components from temporal time-series while keeping the rest of the spectrum. Depending on the frequency components to be rejected, high pass, low pass, band pass, band reject, notch, and comb filters can be applied.

Artifact Correction: EEG is highly sensitive to non-physiological and physiological artifacts, even in controlled laboratory conditions. Among their sources we find subject movements, muscular activation, eyes and eyelid movements, artifacts related to the cardiac activity, and electromagnetic interference such as power line noise. If possible, it is highly recommended to remove or reduce the influence of such nuisance signals.

Channel Reference: Channel referencing enhances the EEG signal to noise ratio (SNR). The choice of the reference channel(s) will depend on the properties of the EEG which are under study (e.g. whether symmetry needs to be fulfilled). Numerical comparison between referencing approaches suggests that average reference best approximates large-scale brain networks [73]. Some of the commonly used references

in EEG analysis are bipolar, linked mastoids, common average, and double banana [74][72].

Epoching: EEG recordings can typically last for minutes or hours. Many analyses and feature extraction processes require these to be split into time windows also known as epochs. Epochs are in general short-time, typically of a few seconds of duration, and in some cases can be considered pseudo-stationary [75].

Epoch Processing and Rejection: Extracted epochs may need further processing to enhance their SNR and to typically remove their offset and trend. After signal cleaning and processing, some epochs may still contain non-physiological artifacts, which should be detected to be discarded from further analysis. The methodology to detect artifacts depends in general on the statistical properties of the artifacts themselves. A simple amplitude threshold that marks epochs whose maximum absolute amplitude crosses the threshold of what is considered as non-physiological is valid in many cases.

Signal Decomposition: The preprocessing stage may require the signal decomposition of EEG. Independent and Principal Component Analysis (ICA, PCA) are commonly used techniques [76]. Independent component analysis, for example, separates the n-channel EEG signal into n additive independent components (IC), assuming that the components are non-Gaussian signals and that they are statistically independent from each other. Principal Component Analysis is generally used for dimension-reduction. It is capable of finding a number of principal components (PC) smaller than n that still contains most of the information of the multichannel EEG signal. PCA uses orthogonal transformations to find maximal data variability at each individually calculated PC.

1.4.3 EEG Features

Once the EEG signals have been processed, they can be used to compute features, aiming to extract meaningful information within the temporal EEG series that may explain its underlying physiological process. Many feature extraction techniques exist, in general involving transformations of

the temporal EEG epochs into other domains. In this section we describe the most relevant features used in EEG analysis.

Event-Related Potentials

Event-Related potentials (ERPs) measure the temporal brain response time-locked to a specific sensory, cognitive, or motor event [77]. The amplitude of the elicited potentials is typically a few micro-volts and therefore not visible within a single epoch. ERPs are extracted by the averaging of multiple trials time-locked to the same event. This averaging process minimizes interferences and background brain activity while the underlying ERP persists. The result is a series of positive and negative deflections that are characterized by their latency and amplitude. ERPs are widely used in clinical and cognitive neuroscience.

Spectral Analysis

Fourier-transform-based spectral EEG analyses stand on the decomposition of EEG time-series into a finite number of sinusoidal components. By studying these sinusoidal waveforms it is possible to analyze the amplitude, frequency and phase of brain rhythms. In computational neuroscience the Fourier transform (FT), and in particular its algorithmic implementation known as fast Fourier transform (FFT) [78], have been largely used for the frequency analysis of EEG time-series. The Fourier transform-based approaches assume the signal to be stationary ignoring any time-varying spectral content within the calculation window. Then to overcome this limitation, the EEG series are split into short-time sequences where EEG rhythms are considered to be pseudo-stationary. To calculate the total spectral response of an EEG sequence the average spectral response calculated at window level is performed [79].

The fact that EEG signals are non-stationary limits the efficacy of Fourier-based methodologies. Wavelet-based spectral analysis is less dependent on the window length, being capable of detecting smaller frequency changes not identified by Fourier-transform based methodologies [80]. A Wavelet transform (WT) decomposes the EEG series into a set of basis functions called wavelets. These are obtained by shifts, dilatations and contractions

of a waveform called mother-wavelet. Wavelets are capable of integrating temporal and frequency information. An optimal shifting, scaling and mother wavelet parameterization is in consequence crucial to achieve solid results.

Connectivity Analysis and Synchronization

As previously explained, EEG electrodes measure the electrical signals produced by large numbers of synchronized neural ensembles that produce local field potentials. These neural ensembles do not work in isolation and influence one another. The relationship between recorded local field potentials, and more generally between brain regions, is studied by means of synchronicity and connectivity. In this section we provide an overview of the most relevant methodologies used to assess signal correlations between EEG electrodes [81]. These metrics provide valuable information for the understanding of the ongoing neural dynamics and are widely used for the characterization of abnormal brain activity. In Chapters 3 and 4 we propose new methodologies, based on echo-state networks, for EEG feature extraction and classification, which exploit the connectivity and synchronization between EEG channels.

The Intersite Phase Clustering (IPC) follows the assumption that the synchronization is produced by a clustering of phase values at each time-frequency point. IPC measures phase relationships between two electrodes over time by computing their average angle differences. It requires the phase differences at each time-frequency point to be similar along trials.

The Phase Lag Index (PLI) assesses functional connectivity from EEG recordings by measuring the asymmetry of the distribution of phase differences between two EEG channels [82].

The Mutual Information (MI) detects the shared information between electrodes. Its concept is linked to that of the entropy of a random variable. It is capable of detecting both linear and nonlinear interactions by analyzing the joint probability distribution of the signal coming

from two electrodes. In spite of its dynamical capabilities, MI numerical results are difficult to interpret as they do not differentiate between positive and negative relationships between electrodes.

The Granger Causality (GC) is a statistical test for assessing if the signal from one electrode can forecast that of another. The application of the Granger causality assumes that the analyzed signals are stationary in terms of their covariance if the variance in one electrode can be predicted by the variance in another electrode earlier in time. Its main advantage lies in its ability to establish the direction of a connection between two brain areas.

The Synchronization Likelihood (SL) is an estimate of the dynamical dependencies between two electrodes that is closely related to the concept of generalized synchronization, therefore accounting for nonlinear dependencies between EEG channels [28].

The Cross-Frequency Coupling (CFC) measures the dynamic interaction between oscillations among different brain rhythms. The two main forms of CFC are phase amplitude coupling (PAC), and phase-phase coupling (PPC). In PAC (also called nested oscillations) the phase of the lower frequency oscillation (nesting) drives the amplitude of the coupled higher frequency oscillation (nested), which results in the synchronization of the amplitude envelope in faster rhythms with the phase in slow rhythms.

The Magnitude-Squared Coherence (MSC) is a stationary metric of the correlation in the frequency domain between a pair of electrodes. Its cross spectral density-based analysis delivers the degree of likelihood between them normalized in the 0-1 range.

Dynamical EEG Analysis and Signal Complexity

The brain is a sophisticated system that produces non-stationary multivariate complex dynamics. The nature of the brain therefore advocates for the use of techniques capable of characterizing complex dynamics in EEG time series. Recurrent neural networks, and in particular echo-state networks, are capable of decoding complex temporal dynamics. In this section we present the most used approaches to characterize complexity in the EEG.

The Lempel Ziv Welch (LZW) algorithm is a universal lossless data compression algorithm that measures the repetitiveness of detected subcomplexes after EEG binarization.

The Entropy is a metric that measures the amount of information conveyed by an EEG sequence. Many forms of measuring entropy exist, among which the ones most used in EEG analysis are permutation, sequence and multiscale entropy.

The Fractal Dimension provides a metric of complexity comparing scale changes in fractal patterns.

1.5 Steady State Visual Evoked Potentials

SSVEPs are a resonance phenomenon that can be measured in the EEG, elicited when gazing at a repetitive visual stimulation source (RVS). During SSVEPs, the neural oscillatory activity synchronizes with the RVS, more prominently in the primary visual cortex. As a consequence, SSVEP components in the EEG match the RVS frequency and its harmonics, resulting in an energy increase at these frequencies that is phase-locked with the stimulation [83]. SSVEP is mainly considered a steady-state stationary response.

In this Thesis we propose a novel methodology for characterizing a brain evoked response, known as State Visual Evoked Potentials (SSVEPs). We have developed a new methodology using echo-state networks that proved to be capable of accurately detecting SSVEPs. This work is presented in Section 3. In this section we describe the SSVEP phenomena and the SSVEP dynamics that can be measured in the EEG. We summarize state-of-the-art methodologies for SSVEP dynamics characterization, ending up with the most relevant SSVEP applications in cognitive and clinical neuroscience.

Figure 1.10 depicts the average spectral response over various stimulation trials for one subject while gazing at a 12 Hz RVS (red) compared to periods with no visual stimulation (blue). An energy increase at the stimulation frequency (12 Hz) and its second harmonic (24 Hz) is clearly observed during visual stimulation. However, a few studies have suggested that SSVEP dy-

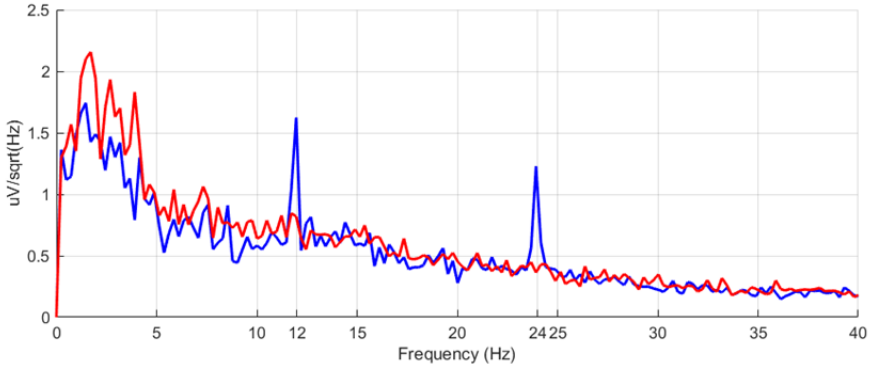

FIGURE 1.10: EEG spectrum during 12Hz visual stimulation (red) and non-visual stimulation (blue).

namics may be richer than a simple resonance effect. SSVEP bursts have been reported to show patterns of large scale synchronicity [84]. In high frequency SSVEPs, after the stimulation onset, a short-time transient response ($<$ 500ms) has been seen to exhibit an increase in delta and theta power over fronto-central and occipital regions [85].

1.5.1 SSVEP Response Variability

SSVEP amplitude response and phase alignment have been proved to be subject and age-dependent [86]. One of the factors that influences the strength and spatial distribution of SSVEP the most is the stimulation frequency [87]. Stimulation source properties such as color, stimulation pattern or luminosity also affect SSVEP dynamics [88]. Recent studies have demonstrated that the SSVEP response can be enhanced through neurofeedback training. Subjects who were able to decrease their alpha power showed a statistical significant strengthening of their later SSVEP response [89].

In SSVEP-based applications where a good detection performance is necessary, as in brain-computer interfaces (BCI), the RVS should be personalized. In practice, the stimulation frequencies that elicit the response with the larger amplitudes are selected during a calibration process. In Figure

FIGURE 1.11: AsTeRICS project participant using a 2-degree of freedom SSVEP-based BCI application

4.11 a spinal cord injury patient participating in AsTeRICS project [90][91] uses a 2-degree of freedom BCI application. AsTeRICS goal was to create flexible communication solutions for people with severe motor disabilities. Within the framework of AsTeRICS, the SSVEP data analyzed and presented in Chapter 3 was recorded.

1.5.2 SSVEP Detection

Many feature extraction techniques are used for the characterization and detection of SSVEPs [92][93][94]. These techniques exploit the steadiness and stationarity of the response, studying the resonance effect induced at the stimulation frequency and its harmonics. The most popular feature extraction approaches are listed below.

Power Spectral Density Analysis (PSDA)

PSDA-based approaches use the power spectral density estimation, e.g. the Welch method [79], to convert the temporal SSVEP response into the spectral domain. These techniques monitor the phase and amplitude at the frequency bins corresponding to the stimulation frequency and its harmonics. Typical approaches evaluate the power ratio between the frequencies

of interest and neighboring frequency bins. [95]. The rationale of this approach can be easily understood looking at the average spectral response during RVS as displayed in Figure 1.10.

Canonical Correlation Analysis (CCA)

Canonical Correlation Analysis is a multivariable calibration-less statistical method to calculate the maximal correlation between two multi-channel signals. CCA finds the weight that maximizes the correlation between a multi-channel SSVEP time-series and a vector space formed by a set of sine-cosine signals at the stimulation frequency and its harmonics [96]. CCA-based techniques have proved to outperform other methodologies in terms of detection accuracy, having reported information transfer rates larger than 150 bits per minute [97].

Multivariate Synchronization Index (MSI)

MSI is a multichannel calibration-less method for frequency detection. MSI characterizes the synchronization between a multichannel SSVEP time-series and reference signals synthetically generated set of sine-cosine series at the frequencies of interest [98]. This method has reported excellent performance, especially for short data length and a small number of channels.

Least Absolute Shrinkage and Selection Operator - LASSO

LASSO is a regression method that performs both variable selection and regularization. LASSO penalizes the absolute value of regression coefficients in order to enhance detection accuracy. LASSO computes the linear regression between the SSVEP time-series and reference signals at the stimulation frequency and its harmonics. This method yields to robust detection when shorter time windows are used [99].

Double-Partial Least-Squares - DPLS

DPLS is a novel training-free approach consisting of a double-layer of partial least-squares. The first layer serves as spatial filter while the second acts as feature extractor [100].

1.5.3 Applications

SSVEP response is analyzed in many paradigms both in cognitive and clinical neuroscience [101]. The most popular SSVEP-based applications are summarized below.

Brain Computer Interfaces

SSVEPs are an excellent choice for the construction of brain computer interfaces (BCI). BCI provides a direct communication pathway connecting the brain to a computer or other external device, and therefore not relying on normal action pathways through peripheral nerves and muscles [102]. This fact makes BCIs the ideal approach for assistive technologies (AT) that aim at overcoming motor limitations. SSVEP-based BCIs offer two main advantages compared to other modalities: they have a larger information transfer rate, and they require a shorter calibration time [103]. A typical SSVEP-based BCI system with N degrees of freedom employs N independent light sources with different visual patterns. Each light source is then associated with a particular action of the BCI system. When the user wants the system to perform a specific action, he/she should therefore gaze at its associated light source.

Cognitive Psychology

Attention
SSVEP response has long been used as an index of visual-spatial selective attention [104]. An enhancement in SSVEP amplitude has proved to be attention-driven, and is more prominent in occipital and temporal areas [105][106].

Perception
SSVEPs have also been successfully applied to the study of human body perception. SSVEP amplitude differences were observed when presenting images of bodies with respect to objects [107]. SSVEP response linked to face recognition has been used to study socio-emotional perception [108].

Working Memory

Differences in SSVEP response were found when performing working memory tasks at both low and high demand [109]. Age is generally accompanied by a decline in memory performance. The 13 Hz SSVEP associated with a spatial working memory task has been studied in statistical populations split into midlife (40-60 years old) and elder (61-82 years old) groups. Evidence of age-related under-activation in frontal regions has been observed, suggesting an age-related decline in working memory performance [110]. Concurrently, power differences in SSVEPs in the alpha and gamma frequency range have proven to be associated with age and cognition, and thus can be used to examine cognitive status in old age populations [111].

Clinical Markers

Autism
Low-level visual processing is atypical in autism spectrum disorders (ASDs). SSVEP amplitude response over a wide range of stimulation frequencies, along with its topographical distribution, have been used to characterize the ASD population [112][113].

Schizophrenia
A reduction in neural activity at the alpha band has been reported in patients suffering from schizophrenia. Concurrently, SSVEP studies have provided strong evidence of early-stage visual processing deficits in schizophrenia [114]. When SSVEP responses are elicited within the alpha range, the occipital deficit in alpha power was partially reverted, but the frontal deficit persisted [114].

1.6 Attention Deficit Hyperactivity Disorder - ADHD

Attention-Deficit Hyperactivity Disorder (ADHD) is one of the most common neurodevelopmental disorders in childhood. EEG has been used for decades for the characterization of abnormal neural activity in ADHD children [115]. Given ADHD diagnosis uncertainties, medication side effects, and how it is applied, ADHD research has recently moved to the development of biomarkers that support ADHD clinical diagnosis. In this Thesis we propose a novel ADHD biomarker based on echo-state networks, work that is presented in Chapter 4. In this section we present ADHD and its

symptoms. We briefly introduce how it is diagnosed and potential treatments. We conclude with a review of state-of-the-art ADHD EEG biomarkers.

ADHD is characterized by inattention, distractibility, hyperactivity and impulsivity [116]. In the USA, ADHD was conceptualized as a pathological disorder in the year 2000 in the 4th edition of the Diagnostic and Statistical Manual of Mental Disorders (DSM-IV) [117]. DSM-IV has been used since in the USA and the rest of the world for formal ADHD diagnosis until it was replaced by its 5th edition (DSM-V) in 2013 [118]. According to DSM criteria the prevalence rate of ADHD is estimated between 5-7% [119]. The DSM equivalent in the EU is the International Statistical Classification of Diseases and Related Health Problems (ICD) [120], with an estimated 1-2% prevalence rate. Three main subtypes of ADHD are diagnosed:

Predominantly hyperactive/impulsive subtype (ADHD-H): predominantly hyperactive or impulsive symptoms with few or no inattentive symptoms. This is the least frequent ADHD subtype.

Predominantly inattentive subtype (ADHD-I): mainly inattentive symptoms with few or no hyperactive symptoms.

Combined subtype (ADHD-C): both inattentive and hyperactive symptoms.

The male-to-female gender ratio indicates that ADHD is more common in boys. ADHD is in general diagnosed at an early age and its symptoms clearly decline with age. Up to 80% of children grow out of ADHD in adulthood [121], a fact that supports the hypothesis of a maturational lag. ADHD symptoms have a severe impact on the lives of children, negatively influencing their academical performance and their social and familiar relationships.

1.6.1 ADHD Diagnosis

ADHD diagnosis is in general assessed based on 1) physical examination of the child, 2) interview with the child, and 3) interviews with parents and teachers. The symptoms must be consistent, persistent and negatively affect behavior, academic performance and social interactions.

At least six of the following symptoms are required in order to be diagnosed with inattentive ADHD following DSM-V.

1. Difficulties sustaining attention and remaining focused during play activities, lectures, conversations or reading. Gets bored easily.
2. Absence and distraction when listening or being spoken to.
3. Difficulty to follow instructions and easily sidetracked.
4. Task and activity planning and organization difficulties.
5. Forgetfulness in daily activities.
6. Daydreams and becomes easily distracted.
7. Reluctance to engage in tasks that require sustained mental effort.
8. Loss of daily items (telephone, keys, school materials).
9. Misses important details or makes careless mistakes in daily activities, homework and tests.

At least six of the following symptoms are required in order to be diagnosed with hyperactive ADHD.

1. Squirms in seat or taps hands or feet.
2. Unable to remain quietly seated.
3. Talks unreasonably.
4. Difficulties in waiting in line.
5. Often interrupts other children's conversations or activities.
6. Unable to be still for prolonged time.
7. Unable to engage in leisure activities quietly.
8. Restless behavior, frequently runs impetuously when inappropriate.
9. Inability to wait for turn in a conversation.

Figure 1.12 shows a multidimensional space of ADHD symptoms [121]. As pointed out by the scientific community, ADHD assessment is subjective and heavily biased towards personal practice and experience, which leads to an intrinsic risk of mis- and over-diagnosis [122][123][124]. Besides, inattention and impulsivity symptoms are not unique to ADHD and also appear in other mental disorders such as anxiety or depression.

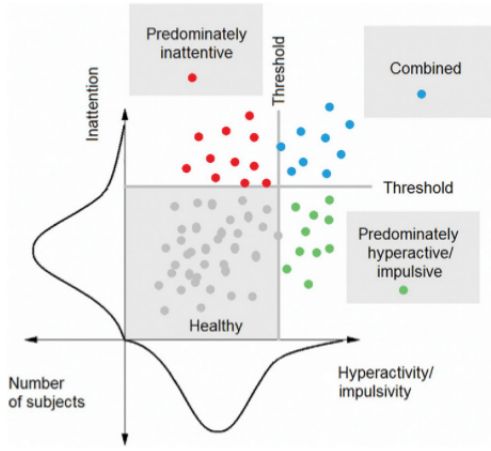

FIGURE 1.12: Multidimensional space of ADHD symptoms.

Finding solid quantitative evidence of neuro-psychophysiological dysfunction in the ADHD population has become one of the most relevant challenges in neuroscience research in the last decades. A robust physiological marker for ADHD is necessary to further understand its underlying neurophysiological mechanisms and will potentially help in a more accurate diagnosis.

1.6.2 The Hypo-Arousal Theory

Arousal is defined as the psychological state of being awake or reactive to stimuli and has long been considered a pathogenic factor in ADHD [125]. The hypo-arousal theory is based on the principle that the ADHD population looks for self-stimulation in order to achieve normal arousal levels

through excessive activity. Arousal deficits and structural alterations in regions involved in modulating arousal and vigilance [126] are believed to be derived from dopamine deficiencies [127]. This is the hypothesis followed in this Thesis to propose a novel EEG-based biomarker as presented in Chapter 5.

Other hypotheses such as the cognitive-energetic model [128] did not focus on underarousal per se, but rather in the difficulties in arousal management. The cognitive-energetic model proposes that ADHD deficits are due to a more unstable energetic pool formed by three interrelated components: arousal, activation, and effort. Following this approach, arousal instabilities are suspected to be affected by the characteristics of the task and thus larger during highly demanding activities.

1.6.3 ADHD Treatment

ADHD is mainly treated with medication, psychotherapy, behavior therapy, and often a combination of them. For over 50 years and increasingly since the 1990s, medications for ADHD are mostly based on stimulants (i.e. amphetamine or methylphenidate) that block the dopamine and noradrenaline pathways [129]. Even though they are considered as safe drugs, they have frequent side effects such as appetite suppression, abdominal pain, insomnia, headache, and anorexia [130]. However, there is no knowledge on which medication improves symptoms with lower side effects. They are currently applied in a "trial and error" manner for each diagnosed child [131]. Recent longitudinal studies report that stimulant medication, behavior therapy or multimodal treatments in ADHD have limited long-term beneficial effects [132]. Alternative treatments have been proposed for ADHD such as neurofeedback, transcranial or magnetic stimulation. Their efficacy is nevertheless still under investigation.

1.6.4 ADHD EEG Markers

In recent years electroencephalographic measures have been widely used to report neurophysiological abnormalities in ADHD children [133]. Despite the great advances in the last decades, state-of-the-art ADHD EEG features do not support their use as a stand-alone diagnostic tool [134], although present developments anticipate its utility in the clinical setting

[115]. EEG biomarker discovery, therefore, remains a hot research topic. In this section we present a summary of EEG features that can potentially be used in decision support systems aiming at supporting ADHD diagnosis.

Stationary ADHD Characterization

The most reported pattern found in ADHD is an excessive power in slow waves, located in front-central regions [135]. EEG slow wave enhancement has been traditionally linked to hypo-arousal brain states [136]. These power abnormalities found when comparing ADHDs and their age matched control group are usually found in the theta band [137].

Theta power increase has been broadly reported to be accompanied by power deficits in fast waves, usually in the Beta band [133]. Theta-beta ratio (TBR), which combines slow activity power increase and fast activity power decrease, has long been used as ADHD biomarker [138]. The US Food and Drug Administration (FDA) approved the Neuropsychiatric EEG-Based ADHD Assessment Aid (NEBA® system), which uses the theta-beta ratio to support the diagnosis of ADHD [135]. However recent studies failed to replicate TBR discrimination performance between ADHD and healthy controls suggesting its inaccuracy in ADHD prediction [139].

TBR may be explained by a broadband brain activity slowing in ADHD children. This slowing is distinctly manifested in the alpha band, characterized by a dominating frequency known as peak alpha frequency (PAF). A theta power increase may reflect individuals with slow alpha peak, shifted towards the theta band, in addition to real increased theta activity. Several studies report PAF slowing in ADHD children [140][141].

Dynamic Characterization of ADHD Patterns

Increased entropy in slow rhythms (delta and theta) along with decreased complexity in alpha has been observed in ADHD during the performance of continuous performance tasks (CPT) [142]. During eyes-closed resting state chaotic dynamics, calculated using multifractal singularity spectrum and Lyapunov exponents, exhibited lower entropy in ADHD subjects in the prefrontal cortex [143]. During a visual cognitive task, LZW complexity scores were significantly higher in control subjects, with the maximum

value in the anterior region [144]. EEG complexity alterations suggest that cortical activation may not be enough to meet the cognitive requirements of highly demanding attention tasks [145]. A new dynamical ADHD biomarker based on echo-state networks is presented in Chapter 4.

1.7 Thesis Organization

This Thesis is organized as a compendium of three publications. They cover specific topics and can be seen as independent studies. Chapters 2, 3 and 4 contain these articles, which are either accepted for publication or under peer review.

In the second chapter we present "Detection of Generalized Synchronization Using Echo State Networks", an article published in the journal Chaos in March 2018. The analysis of preliminary results after using ESN in EEG data suggested that the network was actually detecting complex synchronization between EEG channels. This hint led us to an exploratory work in which using in-silico signals we aimed to study in detail their capabilities for the detection of chaotic synchronization. Two chaotic attractors were sequentially coupled and de-coupled, constructing a continuous temporal series consisting of concatenated sequences of periods of generalized synchronization alternating with periods of no synchronization. As explained in Section 1.3, generalized synchronization is a type of chaotic synchronization with applications in communications and biological systems. ESNs proved to be capable of detecting generalized synchronization with great accuracy, even in the presence of relatively high noise levels.

In the third chapter we present "Echo State Networks Ensemble for SSVEP Dynamical Online Detection", a work submitted to PLOS ONE in June 2018 and currently under revision. Steady-state visual evoked potentials (SSVEPs) are a resonance phenomenon measured in the EEG that appears when gazing at a visual stimulation source. This phenomenon is usually considered to be purely stationary. Using ESN we studied the dynamical characteristics of the SSVEP response and proposed a novel non-stationary methodology for SSVEP detection based on an ensemble ESN with potential applicability in brain-computer interfaces. The proposed methodology outperformed state-of-the-art stationary approaches in terms of accuracy

and information transfer rate.

In the fourth chapter we present the work "Hypoarousal non-stationary ADHD biomarker based on echo state networks", submitted to the Journal of Neuroscience Methods in June 2018 and currently under review. In this work we successfully propose a novel EEG biomarker for one of the most common neurodevelopmental disorders of childhood, namely attention deficit hyperactivity disorder (ADHD). The proposed biomarker is capable of quantifying changes in non-stationary EEG patterns between two cognitive states: normal and low arousal conditions. These changes revealed to be abnormal in the ADHD population.

Finally in the fifth chapter we finish with a results discussion, conclusions, key findings and prospects for future work.

2 Detection of generalized synchronization using echo state networks

Ibáñez-Soria D, Garcia-Ojalvo J, Soria-Frisch A, Ruffini G. Detection of generalized synchronization using echo state networks. Chaos. 2018 Mar;28(3):033118. DOI: 10.1063/1.5010285

3 Echo State Networks Ensemble for SSVEP Dynamical Online Detection

Echo State Networks Ensemble for SSVEP Dynamical Online Detection

D Ibanez-Soria[1], A. Soria-Frisch[2], J Garcia-Ojalvo[3], G Ruffini[4]

[1]**D. Ibanez-Soria** is with Starlab Barcelona S.L., Neuroscience Research Business Unit, Barcelona, Spain. david.ibanez@starlab.es.
[2]**A. Soria-Frisch** is with Starlab Barcelona S.L., Neuroscience Research Business Unit, Barcelona, Spain. aureli.soria-frisch @starlab.es
[3]**J. Garcia-Ojalvo** is with the Department of Experimental and Health Sciences, Universitat Pompeu Fabra, Barcelona. jordi.g.ojalvo@upf.edu.
[4]**G. Ruffini**. is with Starlab Barcelona S.L. and Neuroelectrics Corporation, Boston, MA, USA. giulio.ruffini@neuroelectrics.com.

Background:
Recent years have witnessed an increased interest in the use of steady state visual evoked potentials (SSVEPs) in brain computer interfaces (BCI), SSVEP is considered a stationary brain process that appears when gazing at a stimulation light source.

New Methods:
The complex nature of brain processes advocates for non-linear EEG analysis techniques. In this work we explore the use of an Echo State Networks (ESN) based architecture for dynamical SSVEP detection.

Results:
When simulating a 6-degrees of freedom BCI system, an information transfer rate of 49bits/min was achieved. Detection accuracy proved to be similar for observation windows ranging from 0.5 to 4 seconds.

Comparison with existing methods:
SSVEP detection performance has been compared to standard canonical correlation analysis (CCA). CCA achieved a maximum information transfer rate of 21 bits/minute. In this case detection accuracy increased along with the observation window length

Conclusions:
According to here presented results ESN outperforms standard canonical correlation and has proved to require shorter observation time windows. However ESN and CCA approaches delivered diverse classification accuracies at subject level for various stimulation frequencies, proving to be complementary methods. A possible explanation of these results may be the occurrence of evoked responses of different nature, which are then detected by different approaches. While reservoir computing methods are able to detect complex dynamical patterns and/or complex synchronization among EEG channels, CCA exclusively captures stationary patterns. Therefore, the ESN-based approach may be used to extend the definition of steady-state response, considered so far a stationary process.

Highlights—
- We present a novel SSVEP dynamical detection approach based on ESN.
- This is the first time ESNs are applied to SSVEP based BCI systems.
- We provide experimental validation of proposed methodology.
- Experimental results indicate non-stationarity in SSVEP patterns.

Keywords— Reservoir Computing, BCI, SSVEP, Echo State Networks, EEG, Dynamical Systems, Canonical Correlation Analysis

I. Introduction

A Brain Computer Interface (BCI) provides a direct communication pathway connecting the brain to a computer or other external device. BCIs do not rely on the brain's normal action pathways through peripheral nerves and muscles, making them an ideal technology for systems assisting or repairing human cognitive or sensory-motor functions [1]. Different modalities for the realization of BCI exist; the most commonly used ones being motor imagery, P300, and Steady State Visual Evoked Potentials (SSVEP) [2]. SSVEP-based BCIs offer two main advantages [3]: i) they have a larger information transfer rate, and ii) they require a shorter calibration time.

Many SSVEP-based BCI systems rely on a protocol where the subject decides voluntarily when to interact with the BCI application. When the system detects the user's intention to perform an action, the visual stimulation is presented during a short time period. A typical SSVEP-based BCI system with N_s degrees of freedom employs N_s independent light sources flickering at different frequencies. Each light source is associated then to a particular action of the BCI system. Therefore, when the user wants the system to perform a specific action, he\she shall gaze at its associated light source. Detection methodologies aim at determining immediately after the short-time stimulation period which of the stimulation frequencies in the BCI set-up elicited a visual evoked response.

Steady-state visual evoked potentials, which appear when a person gazes at a flickering light source, are measured by electroencephalography (EEG). The flickering frequency of the light source can range from 1 to 100 Hz [5]. SSVEPs appear as oscillatory components in the user's EEG matching the stimulation frequency and its harmonics, they are mainly observed in the primary visual cortex, and are characterized by an energy increase that is phase-locked with the visual stimulus [5]. The SSVEP response is a subject- and stimulation-dependent phenomenon determined by the stimulation

frequency, its intensity, color, and duty cycle [2].

The brain is a complex, dynamical system that generates non-stationary EEG patterns [6]. This complexity limits the efficacy of non-dynamical feature extraction and classification methods. In this context, it is worth mentioning that the study of transient responses of complex dynamical systems has recently led to the proposal of a new information-processing approach, known as Reservoir Computing (RC). This paradigm opens a wide variety of possibilities for EEG analysis in general and for real-time applications, such as BCI in particular. Although RC techniques have been applied with excellent results to motor imagery [7], they have never been used for SSVEP detection before (to our best knowledge). This is probably due to the assumed stationary nature of the SSVEP response. In this work we aim to exploit the capabilities of reservoir computing for online SSVEP detection. The performance of the proposed RC approach is compared to standard canonical correlation analysis (CCA), which has shown better performance than traditional fast Fourier transform-based spectrum estimation methods [8].

The paper is structured as follows. In section 2 we provide an overview of reservoir computing. We present the new methodology based on RC in section 3. In section 4 we describe our experimental protocol, and in section 5 we provide results for the two approaches under comparison. We conclude with a discussion in section 6.

II. Reservoir Computing

Artificial neural networks have been extensively used for the analysis of stationary problems in computational intelligence. These architectures are well understood due to their feed-forward structure and non-dynamical nature. It is in general not possible to detect temporal dynamics using feed-forward structures. A possible temporal generalization strategy is to add recurrent connections, which allow the system to encode time-dependent information by providing the network with fading memory and transforming it into a complex system [9]. In contrast with feed-forward networks, neural networks whose activation is fed unidirectionally from input to output, recurrent neural networks (RNNs) present at least one cyclic path of synaptic connections, implementing a nonlinear dynamical system [10]. Dynamical systems are commonly used to model non-stationary physical phenomena. These models are extensively used in a wide variety of fields including finance [11], economics [12] and physiology [13].

Since the early 1980s, a wide variety of approaches for adaptive learning in networks with recurrent connections have been proposed [14]. Training RNNs has traditionally been more complex and computationally more expensive than training feedforward neural networks. Additionally, cyclic connections can provoke nonlinear bifurcations leading to drastic changes in its behavior [15]. Echo State Networks (ESN) [16] and Liquid State Machines [17] together constitute a new approach towards training and applying Recurrent Neural Networks, grouped under what came to be known as reservoir computing (RC). RC is based on the principle that supervised adaptation of all interconnection weights in RNNs is not necessary: training a supervised readout from the reservoir is sufficient to obtain excellent performance in many tasks [18]. This approach has certain analogies with kernel methods in ML, with the reservoir performing a nonlinear high-dimensional projection of the input signal for discriminating samples that are not linearly separable in the original space. At the same time, the so-called dynamical reservoir, which is formed by a randomly connected network of varying number of nodes, serves as a memory providing the temporal context [19].

The global structure of an RNN is depicted in Fig. 1. Following the nomenclature and model adopted by Jaeger in [10] we consider a network of K input units, N internal units, and L output units. Input, internal and output connection weights are defined respectively by the connection weight matrices W^{in}, W and W^{out}, $and\ back$-projection weight matrix by W^{back}. In ESN-based supervised training the random input (W^{in}), internal (W) and back-propagation weights (W^{back}) matrices form the dynamical reservoir (DR). A DR is an echo state network if it presents the echo state property. This property states that the current state of a network, which is running for an infinite time, is uniquely determined by the history of the input and the teacher-forced output (i.e. the initial state of the RNN does not matter, since it is forgotten). The echo state property has proved to be linked with the characteristics of the reservoir, with the input signals and with the input and back-propagation weights [20,21,22]. The weight matrix is usually characterized by its spectral radius, defined as the largest absolute eigenvalue of the weight matrix. It is closely connected with the intrinsic dynamical timescale of the reservoir, and is therefore a key ESN training parameter. A small spectral radius leads to a faster RNN response. In most practical applications, a spectral radius below unity ensures the echo state property [23]. Other key training parameters in RC are the input scaling and the model size [23]. The model size is defined by the number of internal units N. Generally, a larger DR can learn more complex dynamics, or a given dynamics with greater accuracy. It is very important however to be aware of the possible over-fitting if a large number of internal units is chosen, which would lead to poor generalization [10]. The input scaling determines the degree of nonlinearity in the reservoir responses. Tasks close to linear require small input scaling factors, while highly nonlinear tasks demand larger input scaling values.

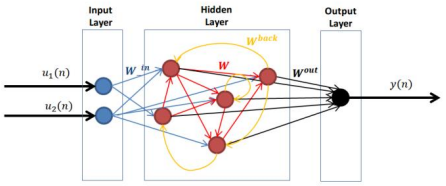

Fig. 1 Echo State Network architecture with 2 inputs and 1 output

III. METHODS

A. Canonical Correlation Analysis

Canonical correlation analysis (CCA) [24] is a multivariable calibration-less statistical method to calculate the maximal correlation between two multi-channel signals. CCA is widely used in statistical analysis and information mining [25, 26]. SSVEP-based BCI systems have largely used CCA-based methods in recent years due to its excellent accuracy and information transfer rate [27, 28]. Given two multidimensional random variables X, Y and their linear transformation $\tilde{x} = w^T X$ and $\tilde{y} = v^T Y$, CCA finds the weight vectors w and v that maximize the correlation between $\tilde{x}$ and $\tilde{y}$. Canonical correlation therefore seeks a pair of linear transformations for X and Y such that when the multidimensional variables are transformed, the corresponding coordinates are maximally correlated [29]:

$$\rho = max \frac{E[\tilde{x}\tilde{y}]}{\sqrt{E[\tilde{x}^2]E[\tilde{y}^2]}} = \frac{w^T XYv}{\sqrt{w^T XXwv^T YYv}} \quad (1)$$

The SSVEP response is characterized by oscillations in the visual cortex matching the stimulation frequency and its harmonics. The performance of a given stimulation frequency f_i is evaluated by computing the canonical correlation between the EEG sequence under evaluation (X) and a reference signal (Y), constructed as a set of sine-cosine series at the stimulation frequency and its N_h harmonics of duration equal to that of the EEG sequence.

$$Y = \begin{pmatrix} \sin(2\pi f_i t) \\ \mathrm{Cos}(2\pi f_i t) \\ \dots \\ \sin(2\pi N_h\, f_i t) \\ \mathrm{Cos}(2\pi N_h\, f_i t) \end{pmatrix} \quad (2)$$

The maximal canonical correlation (ρ_i) is calculated for all N stimulation frequencies (f_i) being tested. In standard CCA the stimulation frequency delivering the largest canonical correlation (ρ) is selected as responsible of eliciting the visual response [30].

B. Reservoir-Computing Ensemble SSVEP Detection

In this section, we propose a novel approach for extraction and classification of SSVEP features, based on an ensemble of as many echo state networks as degrees of freedom the SSVEP-based BCI application has. Each ESN is trained to detect the elicited response to a particular stimulation frequency. The proposed approach is able to detect linear and nonlinear patterns in the EEG response, boosting the capabilities of state-of-the-art stationary detection methodologies.

1) Temporal SSVEP Feature Extraction:

SSVEP EEG temporal components are calculated for each of the N_e electrode signals (which are denoted as $x_i(n)$, $i = 1,2,3 \dots N_e$). The SSVEP temporal response at f_i for harmonic K is computed by filtering the raw EEG using a band-pass FIR filter (1 Hz bandwidth) with its central frequency at $K \cdot f_i$. The ensemble response of every harmonic under evaluation is computed by adding the calculated temporal response of each harmonic, obtaining the $x_i^{f_i}(n)$ vector.

2) ESN Construction:

ESNs (one per stimulation frequency) have been configured to have one output node, and as many input nodes as EEG electrodes measure the visual evoked response (N_e). As will be explained in following sections, the optimal number of internal units, spectral radius, and input scaling factor are calculated using three-fold cross validation exhaustive search.

The temporal decomposition of SSVEP components coming from each electrode $(x_i^{f_i}(n))$ feeds the N_e input nodes of the ESN targeting detection of f_i. The proposed ESN detection and classification methodology is applied to an EEG recording acquired during the interleaving of N_s non-stimulation periods followed by N_s stimulation ones, where the visual stimulation is presented at f_i. The function of the ESN is to discriminate visual stimulation periods at f_i from non-stimulation periods or stimulation periods at other frequencies. For this two-class classification problem, during ESN training, the network outputs $(y_{f_i}(n))$ of samples corresponding to stimulation periods at f_i are set to 1, while the output of samples corresponding to non-stimulation periods are set to -1. Therefore, during the ESN recall the associated ESN output is maximized during the visual stimulation period.

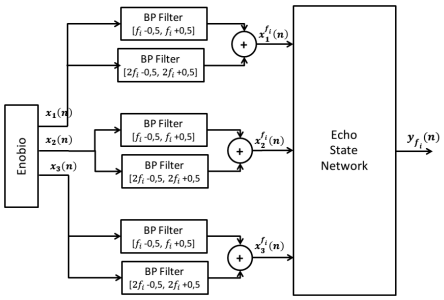

Fig. 2 Proposed RC-based SSVEP Feature Extraction Architecture for the detection of the stimulation frequency f_i.

3) Stimulation Frequency Detection:

SSVEP frequency detection aims at determining which stimulation frequency among the ones under evaluation (f_i, with $i = 1,2 \dots N$) elicited the visual response during a stimulation trial. To achieve this, the RC-based architecture has been designed as an ensemble of N ESNs, where each ESN has been trained for each particular stimulation frequency f_i. The SSVEP response at each frequency (R_{f_i}) is assessed as the difference between the averaged ESN output ($y_{f_i}(n)$) during the stimulation observation window and a baseline sequence prior the stimulation. As the ESN output is maximized during stimulation periods at the trained stimulation frequency, the stimulation frequency with maximal R_{f_i} will be selected as responsible of eliciting the visual response.

IV. Experimental Method

Five Caucasian male subjects S1 to S5 with average age 33.6 years participated in six recording sessions each, where oscillatory visual stimuli were presented at six different frequencies f_i: 12, 14, 16, 18, 20 and 22 Hz. Although a strong SSVEP response can be obtained for stimulation frequencies in the range 5–20 Hz [31], stimulation frequencies below 12 Hz were discarded because the subjects found them uncomfortable. The visual stimuli were presented using stimulation sources consisting of an array of flickering light emitting diodes (LEDs) through a diffusing panel of 100 squared centimeters, developed specifically for this study. Stimulation sources integrated a communication layer through which their stimulation frequency, duty cycle, luminosity and color could be configured. In this study, the LED current was modulated in the form of a squared 50% duty-cycle excitation and with white color for every stimulation frequency.

Each session consisted of one recording per stimulation frequency. In each recording, $N_s = 15$ stimulation trials (duration randomly ranging from 4 to 5 seconds), where the visual stimulus was presented, were followed by the same number of non-stimulation trials (duration randomly ranging from 5 to 8 seconds) with no visual stimulation. Visual stimuli were presented using two stimulation sources next to each other. Higher number of simultaneous stimulation sources, which would reproduce for instance a BCI system of 6 degrees of freedom, were not used because of limitations in the available hardware and stimulus-presentation platform. In our case, one stimulation source was placed on the right of the subject, presenting the stimulation frequency under evaluation, while the one placed on the left presented a frequency randomly selected among the other frequencies used in the experiment. Stimulation sources were separated by approximately 25 cm. The user was comfortably seated at one-meter distance from the stimulation sources and was instructed to look at the stimulation source placed on his right when hearing a beep sound (played one second before the stimulation started). EEG was acquired using an Enobio® recording system at a sampling rate of 250 samples/second from three channels placed in O1, Oz and O2, according to the 10-20 system [32], with the electrical reference placed in the right ear-lobe. Background ambient light remained homogeneous throughout all experimental sessions. The AsTeRICS [33] platform was used to record the EEG streaming data, control the stimulation panels, and trigger the recording.

V. Performance Evaluation and Results

The goal of the performance evaluation is to determine whether RC-ESNs are a suitable tool to be used in practical SSVEP-based BCI applications. To do so its performance is compared to standard canonical correlation detection. Although, as mentioned above, all six stimulation frequencies being tested were not simultaneously presented due to hardware limitations, a BCI system with six degrees of freedom is simulated. In operational conditions the detection methodologies will aim to determine which of the 6 frequencies under evaluation (12, 14, 16, 18, 20 and 22 Hz) is responsible for eliciting the evoked potential after the stimulation trial. Self-paced BCIs require the system to prompt the user for a response and therefore ignore unexpected user input. The performance of such systems is usually measured using the information-transfer rate B [34], which quantifies (in bits per minute) the amount of information reliably received by the system [35]. Denoting the application speed in trials/second by V, the classifier accuracy by P and the number of degrees of freedom of the BCI system by N, the information transfer rate is calculated as:

$$B = V\left[log_2(N) + Plog_2(P) + (1-P)log_2\left(\frac{1-P}{N-1}\right)\right] * 60 \qquad (3)$$

1) Canonical Correlation Analysis:

Recordings have been band-pass filtered using a finite impulse response filter with 250 coefficients and high and low cut-off frequencies set to 1 and 45 Hz, respectively.

The filtering aims to reduce the influence of high amplitude low-frequency components caused by motion artifacts and bad electrode-skin contact, as well as reducing power line-noise interferences. After filtering, stimulation sequences have been extracted and split into shorter observation windows starting at the beginning of the visual stimulation. Maximal canonical correlation has been calculated for each stimulation frequency and its second harmonic. Table 1 presents the detection accuracy and ITR for the 6-degree-of-freedom BCI-system under test in 0.5, 1, 1.5, 2, 2.5, 3, 3.5, and 4-second observation windows. Figure 3 shows the individual ITR and detection accuracy for each participant for the proposed observation windows. Detection accuracy has been proven to increase along with the observation window length, achieving a maximum of 65% in the 4-second observation window. The maximum information transfer rate, 21 bits/minute, was obtained in the 1.5-second observation window. The data shows an important amount of subject variability: while some subjects achieve an excellent detection accuracy and ITR (Subject 3 has 92% classification accuracy for a 4-second observation window and a ITR of 75 bits/minute in 1.5-second windows), others deliver poor classification results (Subject 5 has 23% detection accuracy for 4-second observation windows and a maximum ITR of 6 bits/minute).

2) ESN Parameterization and Stimulation Frequency Detection

ESN networks have been configured to have $N_e = 3$ input nodes and one output node. Input nodes are fed with the filtered signals coming from O1, Oz and O2. The activation function of the network nodes is set to a hyperbolic tangent. A washout duration of 250 samples has been applied.

RC-ESN Optimal Parameterization:

The optimal number of internal units, spectral radius and input scaling has been calculated through exhaustive search. The detection accuracy calculated over 4-second observation windows and 0.5-second baseline has been assessed for every combination of internal units (from 10 to 200), spectral radius (from 0 to 1) and input scaling factor (0.001, 0.01, 0.1 and 1). In order to keep the temporal dynamics, recordings (containing 15 stimulation trials) have been split into three non-overlapping time series consisting of five consecutive stimulation/non-stimulation trials. Cross-validation using the concatenation of two-time series as training set and the remaining series as test set has been employed to evaluate every tuple under test. In each stimulation sequence under evaluation, the frequency maximizing the difference between the average ESN output in the 4-second observation window and the average ESN output in a 0.5-second baseline measured before the stimulation trial is selected as responsible of eliciting the visual evoked response. A spectral radius of 0.7, 140 internal units and 0.1 input scaling factor was found to deliver the best average classification accuracy across subjects (65.4%).

RC-ESN SSVEP Detection:

The previously calculated optimal spectral radius, internal units and input scaling are applied to SSVEP detection in 0.5, 1, 1.5, 2, 2.5, 3, 3.5, and 4-second observation windows using a baseline of 0.5 seconds. Cross-validation as described in Section 5.2.1 above has been used to assess the detection performance at each observation window. The average of three independent iterations has been calculated in order to reduce the random dynamical reservoir construction. Table 1 presents the calculated detection accuracy and ITR, considering the trial duration as the addition of the observation window and the initial baseline duration. Figure 4 presents individual ITR and detection accuracy for each participant. Unlike in canonical correlation analysis, observation window duration does not influence the detection accuracy of the RC-ESN-based detection. Similar average and individual detection performance is achieved for every observation window length under test. Average detection accuracy for every observation window is similar to the maximum accuracy obtained for CCA, in this case in 4-second windows. This fact boosts the maximum obtained ITR that reaches 49 bits/minute in 0.5-second windows.

ESN Parameterization Influence in SSVEP detection:

The spectral radius is intimately connected to the timescale of the reservoir and is a key ESN parameter. The impact of spectral radius is evaluated by setting the number of internal units to 140, the input scaling to 0.1 and computing the detection performance through cross fold validation as described in Section 5.2.1, for spectral radius values of between 0 and 1. Setting the spectral radius to zero kills the recurrence in the reservoir. Since

feedback weights are used, such a zero-spectral-radius system would amount to an IIR filter. Figure 5 shows individual and average detection accuracy performance for different observation windows. The results reveal that performance significantly decreases for a zero-spectral radius system, proving that the system is actually exploiting the within-reservoir recurrence to perform the SSVEP detection. According to Figure 5, the average performance of all observation windows under test shows that average detection accuracy slightly improves along with the spectral radius up to a spectral radius value of 0.7.

The model size, defined by the number of internal units, is also a key training parameter. In general, more internal units can learn more complex dynamics, although it is very important to avoid over-fitting of the training set if a large number of internal units is used. The influence of model size in SSVEP detection performance is evaluated setting the spectral radius to 0.7, the input scaling factor to 0.1 and calculating the detection performance through three-fold cross validation as described in Section 5.2.1, for a number of internal units ranging from 10 to 200. In Figure 5 the detection performance of the model size under evaluation is presented. The results show that average detection performance increases asymptotically with model size.

Table 1 Detection accuracy percentage and ITR (within brackets) in bits / minute

	0.5''		1''		1.5''		2''		2.5''		3''		3.5''		4''	
	cca	esn	cca	esn	cca	esn	cca	esn	cca	esn	cca	esn	cca	esn	cca	esn
S1	17 (0)	77 (77)	36 (9)	80 (55)	52 (19)	84 (47)	58 (18)	84 (38)	66 (20)	84 (32)	68 (18)	86 (29)	76 (20)	91 (29)	76 (18)	86 (22)
S2	19 (0)	40 (13)	28 (3)	40 (9)	39 (8)	42 (8)	44 (9)	42 (6)	54 (12)	42 (5)	62 (15)	39 (3)	67 (15)	40 (3)	69 (14)	42 (3)
S3	28 (6)	89 (108)	74 (70)	93 (81)	90 (75)	93 (61)	88 (51)	94 (51)	94 (51)	92 (40)	92 (40)	90 (32)	91 (33)	91 (29)	92 (30)	90 (25)
S4	16 (0)	44 (18)	22 (1)	53 (19)	32 (4)	53 (15)	43 (8)	53 (12)	44 (7)	57 (12)	51 (9)	53 (9)	53 (8)	54 (8)	66 (12)	51 (6)
S5	23 (3)	52 (29)	32 (6)	49 (16)	22 (0)	51 (13)	21 (0)	49 (10)	19 (0)	50 (8)	23 (0)	48 (7)	28 (1)	44 (4)	23 (0)	44 (4)
Avg	21 (2)	61 (49)	38 (15)	63 (36)	47 (18)	64 (29)	51 (14)	65 (23)	55 (15)	65 (20)	59 (14)	63 (16)	63 (13)	64 (15)	65 (12)	63 (12)

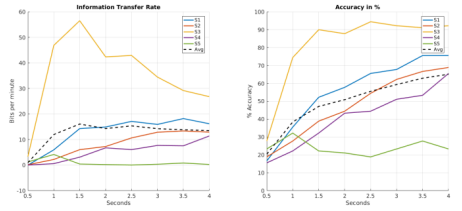

Fig. 3 *Information transfer rate (left) and detection accuracy (right) at different observation-window length using standard CCA detection.*

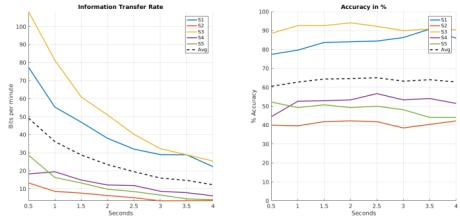

Fig. 4 *Information transfer rate (left) and detection accuracy (right) at different observation-window length using ESN-based detection.*

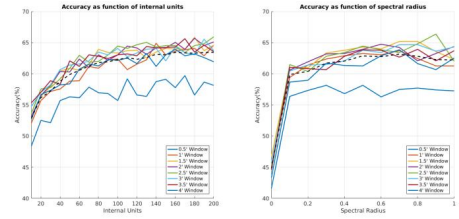

Fig. 5 *Detection accuracy of the ESN-based method as function of the number of internal units (left) and spectral radius (right).*

Individual Stimulation Frequency Detection

SSVEP is a subject-dependent phenomenon in which a given stimulation frequency has proved to range from excellent classification accuracy to random classification among subjects [36]. The feasibility of an SSVEP-based system thus strongly depends on the appropriate individualization of used stimulation frequencies. Table 2 presents the detection accuracy for each stimulation frequency obtained for the observation windows delivering largest average detection accuracy along all stimulation frequencies for CCA and ESN-based methodologies, respectively 4 and 2 seconds. ESN-based methodologies significantly improve the average detection accuracy of subjects 1 and 5, while standard CCA performs better in subject 2 and 4. Both methodologies deliver similar average classification performance for subject 3. Results show that the ESN-based method significantly improves classification in some stimulation frequencies and subjects compared to CCA (subject 1, stimulation frequency 20 Hz) and vice versa (subject 2 stimulation frequency 14 Hz). These classification differences may prove the elicitation of evoked responses of different nature, explaining why stationary and dynamical detection methodologies perform differently. The brain response to a flickering stimulation has traditionally been considered to be a steady-state system, in which the effect elicited is considered to be unchanging in time. In the cases in which reservoir computing outperforms CCA, complex dynamical patterns and/or complex synchronization among

EEG channels may have been detected. The complex nature of the elicited visual stimulation response shall be studied further in order to complete the definition of steady-state visual evoked potentials. In any case, our results indicate that standard CCA and ESN-based methodologies are complementary in terms of SSVEP detection.

Table 2 Detection accuracy percentage of canonical correlation analysis (4-seconds observation window) and proposed ESN-based methodologies (2-seconds observation window)

	Subject 1		Subject 2		Subject 3		Subject 4		Subject 5	
	cca w=4''	esn w=2''	cca w=4''	esn w=2''	cca w=4''	esn w=2''	cca w=4''	esn w=2''	cca w=4''	esn w=2''
12Hz	100	87	100	87	100	100	67	6	67	20
14Hz	93	80	80	33	100	100	80	33	40	53
16Hz	80	80	66	13	100	100	80	87	13	53
18Hz	87	87	46	47	100	87	80	53	6	60
20Hz	53	80	33	13	93	100	53	80	13	87
22Hz	40	93	86	8	60	80	33	67	0	33
Avg	**75**	**84**	**68**	**39**	**92**	**91**	**65**	**50**	**23**	**50**

VI. Discussion And Conclusions

We have presented a reliable SSVEP-detection methodology based on reservoir computing with online capabilities. Its performance has been successfully compared to standard canonical correlation analysis for the construction of a BCI system of six degrees of freedom. The information transfer rate of the hereby proposed approach does not overcome state of the art high-speed SSVEP approaches such as Nakanishi's [39]. However it is limited in terms of degrees of freedom (6 instead of 32), covers a larger stimulation frequency range (from 6 to 22 instead of from 8 to 15) without phase-coding and uses a smaller number of electrodes.

The performance of our proposed ESN-based method proved to be non-dependent from observation window length, delivering similar detection accuracy for windows ranging from 0.5 to 4 seconds (from 61% to 65%). In contrast, CCA showed a strong dependence on the stimulation window duration, with 0.5-second observation windows delivering random classification, and accuracy increasing with window length, reaching a maximum detection accuracy of 65% in 4-second windows. These results highlight the communication capabilities of the ESN-based method, which achieves an average information transfer rate of 49 bits/minute (with a maximum ITR of 108 bits/minute obtained for a single subject), compared with the maximum average information transfer rate of 21 bits/minute achieved by the CCA method. The ESN-based method achieves an excellent information transfer rate for a six-degrees-of-freedom BCI system compared to other state of the art high-rate SSVEP systems [2,37,38].

SSVEP is a subject-dependent technique in which the stimulation frequency defines the classification performance. In this study, a wide range of frequencies ranging from 10 to 22 Hz in steps of 2 Hz is used to simulate a six-degrees-of-freedom SSVEP-based BCI system. Individualized stimulation frequency selection is expected to improve the detection accuracy of both CCA and ESN-based methods. Both methodologies have proved to be complementary in terms of detection accuracy. The ESN and CCA-based methods proved to deliver excellent detection accuracy at different stimulation frequencies. For instance, in our study Subject 5 offered 87% detection accuracy at 20Hz stimulation when using the ESN-based detection methodologies, and near-to-random classification with the CCA-based method. In contrast, Subject 2 showed 80% detection accuracy for CCA-based methods and 33% for the ESN-based technique. A possible explanation for this behavior could be that in different subjects each stimulation frequency may elicit evoked responses of different nature, in terms of their dynamical/stationary characteristics. Specifically, reservoir computing methods are able to detect complex dynamical patterns and/or complex synchronization among EEG channels, in contrast to stationary patterns detected by canonical correlation analysis. The brain response to a flickering stimulation has traditionally been considered to be a steady-state system, in which the effect elicited is considered to be unchanging in time. The hypothesis of complex dynamical activity elicited by visual repetitive stimulation shall be further studied in order to complete, if confirmed, the definition of steady-state visual evoked response.

Acknowledgment

We want to thank all members of the AsTeRICS project consortium; special acknowledgements go to the AsTeRICS users who helped us to test and improve the system. We also kindly thank the developers of the Oger toolbox [40].

References

[1] Shih, J. J., Krusienski, D. J., & Wolpaw, J. R. (2012, March). Brain-computer interfaces in medicine. In Mayo Clinic Proceedings (Vol. 87, No. 3, pp. 268-279). Elsevier.

[2] Zhu, D., Bieger, J., Molina, G. G., & Aarts, R. M. (2010). A survey of stimulation methods used in SSVEP-based BCIs. Computational intelligence and neuroscience, 2010, 1.

[3] Cheng M, Gao X, Gao S and Xu C 2002. Design and implementation of a brain-computer interface.

[4] Dornhege G, Millan J D R and Hinterberger T 2007. Toward Brain-Computer Interfacing (Neural Information Processing). The MIT Press.

[5] Mason S, Bashashati A, Fatoure-chi M and Navarro K 2007. A comprehensive survey of brain interface technology designs. Annals of biomedical engineering, 35(2). 137–169.

[6] Coyle, D. (2009). Neural network based auto association and time-series prediction for biosignal processing in brain-computer interfaces. Computational Intelligence Magazine, IEEE, 4(4), 47-59.

[7] Kindermans, P. J., Buteneers, P., Verstraeten, D., & Schrauwen, B. (2010). An uncued brain-computer interface using reservoir computing. In Workshop: machine learning for assistive technologies, Proceedings.

[8] Lin, Z., Zhang, C., Wu, W., & Gao, X. (2007). Frequency recognition based on canonical correlation analysis for SSVEP-based BCIs. IEEE Transactions on Biomedical Engineering, 54(6), 1172-1176.

[9] Schrauwen, B., Verstraeten, D., & Van Campenhout, J. (2007). An overview of reservoir computing: theory, applications and implementations. In Proceedings of the 15th European Symposium on Artificial Neural Networks. p. 471-482 2007 (pp. 471-482).

[10] Jaeger, H. (2002). Tutorial on training recurrent neural networks, covering BPPT, RTRL, EKF and the" echo state network" approach. GMD-Forschungszentrum Informationstechnik. Lukoševičius,

[11] Giles, C. L., Lawrence, S., & Tsoi, A. C. (1997, March). Rule inference for financial prediction using recurrent neural networks. In Computational Intelligence for Financial Engineering (CIFEr), 1997., Proceedings of the IEEE/IAFE 1997 (pp. 253-259). IEEE.

[12] Kuan, C. M., & Liu, T. (1995). Forecasting exchange rates using feedforward and recurrent neural networks. Journal of applied econometrics, 10(4), 347-364.

[13] Cheron, G., Cebolla, A. M., Bengoetxea, A., Leurs, F., & Dan, B. (2007). Recognition of the physiological actions of the triphasic EMG pattern by a dynamic recurrent neural network. Neuroscience letters, 414(2), 192-196.

[14] Williams, R. J., & Zipser, D. (1989). A learning algorithm for continually running fully recurrent neural networks. Neural computation, 1(2), 270-280.

[15] Jaeger, H.: The “echo state” approach to analyzing and training recurrent neural networks. Tech. Rep. GMD Report 148, German National Research Center for Information Technology (2001).

[16] Martens, J., & Sutskever, I. (2011). Learning recurrent neural networks with hessian-free optimization. In Proceedings of the 28th International Conference on Machine Learning (ICML-11) (pp. 1033-1040).

[17] Martens, J., & Sutskever, I. (2012). Training deep and recurrent networks with hessian-free optimization. In Neural networks: Tricks of the trade (pp. 479-535). Springer Berlin Heidelberg.

[18] Jaeger, H. (2001). Short term memory in echo state networks. GMD-Forschungszentrum Informationstechnik.

[19] Lukoševičius, M., Jaeger, H., & Schrauwen, B. (2012). Reservoir computing trends. KI-Künstliche Intelligenz, 26(4), 365-371.

[20] Manjunath, G., Tino, P., & Jaeger, H. (2012). Theory of Input Driven Dynamical Systems. dice. ucl. ac. be, number April, 25-27.

[21] Buehner, M., & Young, P. (2006). A tighter bound for the echo state property. IEEE Transactions on Neural Networks, 17(3), 820-824.

[22] Yildiz, I. B., Jaeger, H., & Kiebel, S. J. (2012). Re-visiting the echo state property. Neural networks, 35, 1-9.

[23] Lukoševičius, M. (2012). A practical guide to applying echo state networks. In Neural networks: Tricks of the trade (pp. 659-686). Springer Berlin Heidelberg

[24] Hotelling, H.: Relations between two sets of variates. Biometrika. 28, 321–377 (1936)

[25] Hünenberger, P. H., Mark, A. E., & Van Gunsteren, W. F. (1995). Fluctuation and cross-correlation analysis of protein motions observed in nanosecond molecular dynamics simulations. Journal of molecular biology, 252(4), 492-503.

[26] Person, R. S., & Mishin, L. N. (1964). Auto-and cross-correlation analysis of the electrical activity of muscles. Medical electronics and biological engineering, 2(2), 155-159.

[27] Bin G, Gao X, Yan Z, Hong B and Gao S 2009 An online multichannel SSVEP-based brain–computer interface using a canonical correlation analysis method J. Neural Eng.

[28] Chen X, Chen Z, Gao S and Gao X 2014 A high-ITR SSVEP based BCI speller Brain-Comput. Interfaces 1 181–91

[29] Hohreiter, V., Wereley, S. T., Olsen, M. G., & Chung, J. N. (2002). Cross-correlation analysis for temperature measurement. Measurement science and technology, 13(7), 1072.

[30] Hardoon, D. R., Szedmak, S., & Shawe-Taylor, J. (2004). Canonical correlation analysis: An overview with application to learning methods. Neural computation, 16(12), 2639-2664.

[31] Jaeger, H. (2001). The “echo state” approach to analysing and training recurrent neural networks-with an erratum note. Bonn, Germany: German National Research Center for Information Technology GMD Technical Report, 148(34), 13.

[32] Jurcak, V., Tsuzuki, D., & Dan, I. (2007). 10/20, 10/10, and 10/5 systems revisited: their validity as relative head-surface-based positioning systems. Neuroimage, 34(4), 1600-1611.

[33] Ossmann R, Thaller D, Nussbaum G, Pühretmair F, Veigl C, Weiß, C, Morales B and Diaz U, 2012. AsTeRICS, a flexible assistive technology cnstruction Set, 4th International Conference on Software Development for Enhancing Accessibility and Fighting Info-exclusion, Book of Abstracts, 11.

[34] J. R. Wolpaw, N. Birbaumer, W. J. Heetderks, D. J. McFarland, P.Hunter Peckham, G. Schalk, E. Donchin, L. A. Quatrano, C. J. Robinson, and T. M. Vaughan, "Brain-Computer Interface Technology: A Review of the First International Meeting," IEEE Transactions on Rehabilitation Engineering , vol. 8, pp. 164-173, 2000.

[35] Kronegg, J., Voloshynovskyy, S., & Pun, T. (2005). Information-transfer rate modeling of EEG-based synchronized brain-computer interfaces.

9

[36] Ibañez D., Soria-Frisch A. (2013). SSVEP-Based BCI Stimulation Frequency Selection Training and Detection Approaches. Proceedings of the Fifth International Brain Computer Interface Meeting 2013
[37] Chen, X., Chen, Z., Gao, S., & Gao, X. (2014). A high-ITR SSVEP-based BCI speller. Brain-Computer Interfaces, 1(3-4), 181-191.
[38] Wang, Y., & Jung, T. P. (2010). Visual stimulus design for high-rate SSVEP BCI. Electronics letters, 46(15), 1057-1058.
[39] Nakanishi, M., Wang, Y., Wang, Y. T., Mitsukura, Y., & Jung, T. P. (2014). A high-speed brain speller using steady-state visual evoked potentials. International journal of neural systems, 24(06), 1450019
[40] http://www.reservoir-computing.org/organic/engine

4 Non-stationary ADHD marker based on echo-state networks

Non-stationary ADHD marker based on echo-state networks

D. Ibanez-Soria[1], A. Soria-Frisch[2], J. Garcia-Ojalvo[3], J. Picardo[4], G. Garcia-Banda[5], M. Servera[6], G. Ruffini[7]

Background:
Attention Deficit Hyperactivity Disorder (ADHD) is one of the most common neurodevelopmental disorders in childhood. ADHD assessment is subjective and heavily biased towards clinical practice and experience, which leads to high misdiagnosis. Finding solid quantitative evidence of neuro-psychophysiological dysfunction in the ADHD population has therefore become one of the most relevant challenges in computational neuroscience.
New Method:
This study proposes a novel non-stationary ADHD biomarker based on Echo-State-Networks capable of quantifying changes in EEG non-stationary dynamics between low (resting with eyes closed) and normal (resting with eyes open) arousal states. According to the hypo-arousal theory, ADHD population shows arousal deficits and looks for self-stimulation through excessive activity in order to achieve normal arousal levels.
Results:
We successfully verified the hypothesis that measured differences between these two conditions are altered in the ADHD population. Statistically significant differences were found only in theta and beta rhythms. Our neural network discriminates better in the ADHD population, suggesting that differences in EEG patterns between low and normal arousal conditions are larger in the ADHD population.
Comparison with Existing Methods:
Traditionally, ADHD biomarkers have revealed an increase in stationary power in the theta band and a decrease in beta. The non-stationary metric here proposed finds significant differences at the same brain rhythms. Compared to stationary band power, our metric provides larger statistical significance in the data-set under test.
Conclusion
A novel non-stationary ADHD biomarker capable of measuring complex synchronization and non-stationary changes between low and normal arousal conditions has been successfully presented and tested.
Highlights:
-We have successfully proposed a novel non-stationary EEG biomarker for ADHD.
-This biomarker is capable of quantifying changes between low and normal arousal states.
-It has shown statistical significance when comparing ADHD and control populations.
-It was successfully compared to state of the art.
-Echo State Networks have been applied for the first time in ADHD characterization.

***Key Words*—Reservoir Computing, ADHD, Echo State Networks, EEG, Biomarkers**

I. Introduction

Attention deficit hyperactivity disorder (ADHD) [1] is a chronic, pervasive childhood disorder characterized by low frustration tolerance, excessive impulsivity, distractibility, and inability to sustain attention and concentration [2, 3, 4]. It is one of the most commonly diagnosed [2] and investigated [4] neurodevelopmental disorders of childhood. The diagnosis of ADHD is based on the evaluation of 9 symptoms of inattention (IN) and 9 symptoms of hyperactivity/impulsivity (HI) using DSM-IV [5]. ADHD diagnosis is usually stratified in 3 presentations or subtypes: combined (6 or more IN and 6 or more HI symptoms), predominantly inattentive (6 or more IN and less than 6 HI symptoms), and predominantly hyperactive/impulsive (6 or more HI and less than 6 IN symptoms). The diagnosis of ADHD has a high prevalence rate that is estimated between 5% and 7% [6, 7].

Although ADHD is currently considered a neurodevelopmental disorder [8], the diagnostic criteria continue to be based primarily on subjective behavioral assessment derived from parent and teacher reports, interviews, or direct observation.

This work was supported by the Horizon 2020 Program STIPED project (Grant agreement number 731827), the Spanish Ministry of Economy and Competitiveness and FEDER (project FIS2015-66503-C3-1-P and Maria de Maeztu programme, MDM-2014-0370), the Generalitat de Catalunya (project 2017 SGR 1054), and the ICREA Academia program.

D. Ibanez-Soria is with Starlab Barcelona S.L., Neuroscience Research Business Unit, Barcelona, Spain (e-mail: david.ibanez@starlab.es)
A. Soria-Frisch is with Starlab Barcelona S.L., Neuroscience Research Business Unit, Barcelona, Spain, (e-mail: aureli.soria-frisch @starlab.es)
J. Garcia-Ojalvo is with the Department of Experimental and Health Sciences, Universitat Pompeu Fabra, Barcelona, Spain (e-mail: jordi.g.ojalvo@upf.edu).
J. Picardo is with the Universitat Illes Balears, department of pyschology (e-mail: jacopic@gmail.com)
G. Garcia-Banda is with the Universitat Illes Balears, department of psychology (e-mail: ggbanda@uib.es)
M. Servera is with the Universitat Illes Balears, department of psychology (e-mail: mateus@uib.es)
G. Ruffini. is with Starlab Barcelona S.L. and Neuroelectrics Corporation, Boston, MA, USA (e-mail: giulio.ruffini@neuroelectrics.com).

Therefore, as Crippa et al. (2017) point out, the diagnosis is heavily based on the experience and practical knowledge of clinicians. This has at least two important consequences. First, there is a social and scientific concern about the reliability and variability of this approach to diagnosis, and the potential for high probability of a misdiagnosis [9,10]. And, second, although some authors consider that brain structural and functional deficits have been proven to be associated with ADHD [10], there is not a clear consensus about this point. Therefore, finding solid evidence of neuropsychophysiological dysfunction in ADHD has become one of the most relevant challenges in mental health research.

In recent years, electroencephalographic (EEG) measures in resting-state conditions have been widely used to monitor neurophysiological abnormalities in the ADHD population [11]. Most reported findings have shown that the ADHD population presents an increased power in fronto-central regions in low frequencies (typically in the theta band) [12, 13] with decreased power in fast frequencies (typically in the beta band) [14, 15]. Theta/beta ratio (TBR) has long been used as an ADHD biomarker [16]. The US Food and Drug Administration (FDA) approved the Neuropsychiatric EEG-Based ADHD Assessment Aid (NEBA®), which uses the theta-beta ratio of the EEG measured in the central EEG electrode Cz combined with a clinician's evaluation to support the diagnosis of ADHD. NEBA cutoffs for analysis were pre-established and are different for adolescents and children [17,18]. However, not all recent studies could validate the usage of TBR, as a biomarker for diagnosing ADHD. Recent studies documented an insufficient accuracy for TBR and theta power in distinguishing children with ADHD from a control group [11, 19, 20]. Therefore the discovery of novel robust ADHD biomarkers remains a hot research topic.

EEG band-power assessments assume a large degree of temporal stability in brain oscillations. Typically, in EEG analysis the signal is split into short-time epochs that are considered to be pseudo-stationary. Band power is estimated at each epoch and subsequently averaged across them [21]. However, it is well known that the brain is a complex system that generates non-stationary EEG patterns of high dimensionality [22, 23]. Such dynamic, chaotic behavior advocates for the use of non-stationary EEG analysis techniques for EEG feature extraction and classification. Here we apply this approach to reexamine the hypothesis that ADHD is associated with a hypoaroused brain state, suggested by scientific evidence over the past decades. This hypothesis is based on the fact that arousal and attention are related and overlapping concepts [24]. Arousal acts as a modulator of attention levels, with changes in arousal followed by changes in attention [25]. Recent theories, such as the cognitive-energetic model [26], include the concepts of arousal, activation, and alertness as basic mechanisms in ADHD [27, 28, 29].

Following the hypoarousal ADHD theory, our hypothesis is that the magnitude of EEG differences between low attention/arousal states (during eyes closed) with respect to normal attention/arousal states (during eyes open), may be altered in the ADHD population. We test here this hypothesis through the study of band-power stationary features, but also dynamical alterations in the temporal dynamics. To this effect, a novel approach based on recurrent neural networks (RNN) in its reservoir computing (RC) form (echo-state networks) is proposed.

EEG Differences between eyes open (EO) and closed (EC) conditions have been largely reported in the alpha band. Arousal increase during EO with respect to resting state with EC has been associated with a global decrease of EEG alpha levels [30]. Alpha levels are in general substantially reduced in amplitude by eye opening [31] and its regime is characterized by a dominating oscillatory rhythm known as the individual or peak alpha frequency (IAF or PAF). This rhythm is however not strictly monotonic, varying over a range of about 1 Hz [32]. Regarding EO-EC changes in other EEG bands, in the EO condition, reductions of absolute power levels in the delta, theta and beta bands been reported in children. Power topographic changes across the scalp have been also observed in all bands [33].

We hypothesize that the EEG dynamic regimes during interleaving intervals of EC-EO, are discriminated through the application of RC differently for ADHD and healthy subjects. RC has been applied in the past to several EEG feature extraction and classification problems such as brain computer interfaces [34, 35], epileptic seizure [36], prognosis in Parkinson's disease [37] or event detection [38]. In a previous work [39] we have demonstrated the capability of RC to well characterize complex dynamics among EEG channels. In the paper presented herein we employ RC to characterize complex dynamics between EEG channel pairs, within frequency bands, which represent therefore a non-linear connectivity between them. To the best of our knowledge, RC has never been applied as a marker for the dynamic characterization of EEG in ADHD.

II. Reservoir Computing

Artificial Neural Networks (ANNs) are computational models inspired by the structure and function of the brain [40, 41, 42]. Their structure consists of a network of interconnected artificial neurons also known as nodes or units. Artificial neurons transmit signals from one to another along the network simulating the biological synapse process. In practice, artificial neurons receive signals from connected neurons, with a fixed weight (w_i) that is set during the network training process. The activation function of each neuron non-linearly maps the sum of input weighted connections into the signal transmitted to other neurons. Typical activation functions in ANN are the rectified linear unit, the sigmoid, the hyperbolic tangent or the unit step. A representation of an artificial neuron is displayed in Figure 1.

ANNs in general present three stratums of neurons: the input, hidden and output layer. Figure 2 represents a network similar to the one used in this work with 2 input units and one output unit. In the network two input signals $u_1(n)$ and $u_2(n)$ feed the two units of the input layer whose goal is to interface with input

data. Input weights W^{in} map the input nodes into the hidden layer. Internal weights (W) interconnect hidden layer units while output weights (W^{out}) map the hidden nodes into a single output node. Adding loops to the hidden layer (W^{back}) transforms what would otherwise be a standard feedforward network (e.g. multilayer perceptron) into a recurrent network, and allows the model to encode time-resolved information and thus to incorporate memory, converting it into a dynamical system [43].

In the 2000s, reservoir computing (RC) –a new framework for training, understanding and using Recurrent Neural Networks– was proposed independently and simultaneously under the names of Echo State Networks (ESNs) [44] and Liquid State Machines [45]. Reservoir computing is based on the principle that certain structural properties of the network make the supervised training of all weights unnecessary. In particular, if the network obeys an algebraic property known as the echo state property (ESP) only readout connections need to be adapted in a supervised way. The untrained network, whose weights are fixed and randomly generated, is known as the dynamical reservoir (DR) and consists of input-scaling, back-projection and internal weights. The reservoir provides memory while nonlinearly expanding the input signal [46].

The ESP holds if the state of the network asymptotically depends only on the input signal, implying that initial conditions dependencies are lost progressively. In practice, input and back-propagation weights do not affect the echo state property that only depends on the internal weights of the hidden layer. In most applications if the spectral radius of internal weights, calculated as the largest absolute eigenvalue of the adjacency matrix of the reservoir, is kept below one the ESP holds [46], although unlikely exceptions have been reported [47].

According to ESN best practices [46], the most important global-parameters that shall be optimized are the: 1) input scaling, 2) spectral radius, 3) leaking rate and 4) reservoir size. When scaling the network inputs, in practice the same input scaling factor is applied to $u_1(n)$ and $u_2(n)$. The input scaling drives the degree of nonlinearity in the reservoir. Linear tasks require small input scaling factors while complex tasks demand larger input scaling values, easily saturating the nodes and thus transforming them into binary switches. The spectral radius governs the time scale of the reservoir, and thus determines how the influence of inputs remains in the system [48], whereas the leak rate determines the speed of the reservoir to update dynamics. The reservoir size is given by the number of internal units and is in general larger in ESNs compared to other neural network approaches [49]. It has to be large enough to learn the dynamics of the input signals, but not too large so it generalizes well with non-training data. The best approach for output weight training is ridge regression regularization, which removes the requirement of injecting noise in the network inputs to ensure a good generalization [46, 50].

Reservoir computing greatly simplifies the training of recurrent neural networks. The dynamical reservoir is randomly constructed according to selected global parameters. Once the DR weights are fixed, readout connections are learnt using a training input and a teacher-forced output. The network is thus able to efficiently perform tasks with complex temporal information with a low-training cost, since only the readout weights need to be trained.

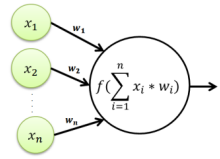

Fig. 1. Artifical Neuron representation

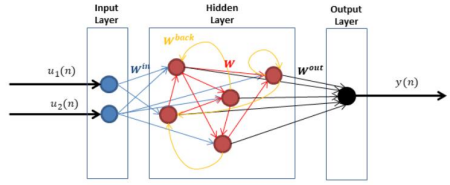

Fig. 2. Recurrent Neural Network Representation.

III. METHODS

A. Participants

52 children aged 7-11 participated in this study. All subjects brought signed parental informed consent and were assigned to one of two groups: clinical diagnosed ADHD group or healthy controls. Children diagnosed with ADHD were recruited from clinical units specialized in pediatric disorders in Palma de Mallorca, Spain. To be considered for the ADHD group, children had to fulfill the following inclusion criteria: (1) being clinically diagnosed with ADHD by a specialist based on DSM-IV criteria (2) not having comorbidity problems of mental retardation, autism, bipolar or psychotic disorders, history of epileptic seizures or any other relevant medical disorder. 28 children were first recruited and assessed into this group, but during the data analysis 7 of them had to be rejected: 3 because they had taken medication 24h prior to the EEG assessment, and other 4 due to noisy EEG recordings. The final ADHD group thus included 21 children: 12 with combined ADHD subtype (11 males and 1 female) and 9 with inattentive subtype (3 males and 6 females).

Healthy controls were selected from standard school age-matched classrooms. The research team met with the schools' principals and tutors, and gave them a dossier (including the informed consent) explaining the project. This dossier was sent home with the kids for their parents. Inclusion criteria for this group were: (1) not having any psychopathology diagnosis, neither mental retardation or learning disorders, (2) not showing behavioral problems nor learning difficulties in class (as asserted by their tutors) (3) not having major family problems

that could interfere with their participation in the study. In the original control sample there were 43 children, but 13 had to be rejected at the final analysis: 7 of them due to academic problems, other 5 due to noisy EEG recordings, and the remaining one due to visual difficulties that prevented him from carrying out one of the experimental tasks. Thus, the final group of healthy controls consisted of a sample of 30 participants. The demographic characteristics of the experimental groups are summarized in Table 1 below.

TABLE I
EXPERIMENTAL POPULATION DEMOGRAPHIC CHARACTERISTICS

	ADHD (n = 21)	Control (n = 30)
Age in years	M 9.6 (SD 1.4)	M 9.3 (SD 1.5)
Male/Female	14 / 7	13 / 17
ADHD C/I	12 / 9	-
Medication (Yes/No)	6 / 15	-

B. Experimental Procedure

The most relevant findings in ADHD biomarkers have been obtained in fronto-central regions [51]. Therefore, in this study we measured the brain activity of the participants in C3, Cz, C4, F3, Fz and F4 using six Ag/AgCl electrodes according to the 10/10 EEG standard positioning system [52]. EEG data was obtained with a Neuroelectrics Enobio® recording system at a sampling rate of 500 Hz. The CMS/DRL electrical reference was placed in the right mastoid. The experimental protocol consisted of a 3-minutes resting-state eyes-open (EO) recording followed by a 3-minute eyes-closed (EC) recording. Participants were instructed to stay still looking at a fixation cross displayed in a computer screen at one meter-distance.

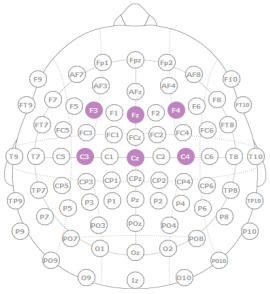

Fig. 3. Position of F3, Fz, F4, C3, Cz and C4 according to 10/20 system

C. ESN-Based Dynamical Synchronization Metric

We now introduce our ESN-based approach aiming at quantifying within-subject dynamical differences between resting EO and EC states at specific frequency bands. The final goal is to employ such performance measure as a surrogate for the differences of EEG signal dynamics, and therefore as a marker for characterizing ADHD patients. The following paragraphs describe the signal processing and analysis pipeline that lead to the computation of the aforementioned biomarker.

Recordings are first filtered using a finite impulse response filter (FIR) at the following bands: theta1 (4-6 Hz), theta2 (6 - 10 Hz), alpha1 (8 - 11 Hz), alpha2 (10 - 13 Hz), beta1 (13-20 Hz), beta2 (20-30 Hz), gamma1 (25-35 Hz) and gamma2 (35-45 Hz). The reference method has a substantial impact on potential measurements. Many reference strategies can be used in EEG analysis, including single electrode reference, linked-ears, linked-mastoids, ipsilateral-ear, contralateral-ear, bipolar references, the tip of the nose or weighted electrode sum [53]. Each modality has its own advantages and disadvantages. In practice, the electrode reference is chosen based on the electrode montage and the characteristics of the feature to be calculated. In this work the average reference of central electrodes C3, Cz and C4 has been used as reference. Frontal electrodes were not selected for referencing as they are likely affected by ocular artifacts. Given we are explicitly taking EO intervals into account, the use of frontal signals in the referencing process could distort the EEG dynamics of other channels.

After referencing, channels C3, Cz, C4, F3, Fz and F4 are split into 10-second epochs with no overlap. Epochs containing samples larger than 75uVs at any channel after de-meaning are rejected, as they are considered to be contaminated by artifacts. Since we are only interested in signal dynamics, each 10-second epoch is individually standardized to mean zero and standard deviation one, removing the amplitude information. EC and EO standardized epochs are then sequentially concatenated creating a continuous EO-EC series for each channel and frequency band. EO-EC series are then smoothed by calculating its envelope using the Hilbert transform [54]. Smoothing removes the possible edge effects produced by the concatenation EO and EC sequences.

Given we want to extract a connectivity measure, ESN networks are fed with the previously presented interleaving temporal dynamics of EO and EC series coming from two EEG channels filtered at the same frequency band. A teacher-forced signal with EO samples set to 1 and EC samples set to -1 is used for training, through which the network learns to distinguish between the two regimes. In previous works we have demonstrated that among other dynamics, ESNs are capable of detecting complex synchronization between two temporal time-series such as generalized synchronization [55]. We thus expect ESN to be capable of detecting synchronization variations among channels between the EO and EC regimes. This is why we will define the resulting biomarker as Channel Dynamical Synchronization Metric (CDSM). We set the ESN node activation function to the hyperbolic tangent, the spectral radius to 0.8, the input-scaling factor to 0.1, the ridge regression coefficient to 0.5, and the number of units in the hidden layer to 500. The network output is low-pass filtered at 5 Hz in order to remove high-frequency components.

We train thus the network to discriminate between EO and EC regimes for every combination of pairs of electrodes at one frequency band. To quantify the discrimination capability we compute the mean squared error (MSE) between the teacher-forced signal and the trained ESN output. We call this measure the Channel Dynamical Synchronization Metric (CDSM). This

feature quantifies how well the network learns to discriminate between the EO and EC conditions at a certain band for a pair of electrodes. The Dynamical Connectivity Index (DCI) of an electrode for a certain band is defined as the average CDSM of its combination with every other electrode. In order to reduce the random effect introduced by the dynamical reservoir construction, we calculate the average CDSM over five independent initialization of the ESN, and use these replicates for further statistical analysis.

D. Stationary Analysis

We performed a comparative evaluation of the newly proposed approach with a conventional stationary spectral analysis. The goal is to obtain a better understanding of the ESN results and to explore non-dynamical changes in the EEG rhythms. The average stationary spectral response and power at frequency bands defined in 2.C is computed for each subject at EO and EC conditions using as reference also the average of C3, Cz and C4. The ratio of the average band power per channel between EC and EO conditions was calculated to measure the stationary differences between these two conditions at subject level for the sake of comparison with the proposed DCI.

E. Statistical Analysis

The statistical analysis aims at measuring if the samples under comparison, belonging respectively to ADHD and control groups are independent and therefore coming from populations with different distribution. According to the Kolgomorov-Smirnoff test result [56] all samples under test do not present a Gaussian distribution. Therefore, we used a nonparametric two-sided Wilkoxon rank-sum test [57], which unlike the t-test does not assume normal distributions, to identify statistical differences between the ADHD and control groups. The null hypothesis was rejected only if the obtained probability value was less than 5%. Statistical significance between groups is here represented by * for probabilities below 5%, ** for probabilities below 1% and *** for probabilities below 0.1%.

IV. Results

A. Dynamical Synchronization Metric Analysis

Figure 4 shows a connectivity representation of the statistically significant p-values ($p<0.05$) obtained when comparing ADHD and control populations. We observe that the synchronization metric proposed here discriminates well between populations, especially in theta and beta bands. Figure 5 and 6 depicts the ADHD (blue) and control (red) CDSM grand averages and standard error of the mean (SEM) in the theta1 and beta1 bands. Given that the CDSM quantifies the error between the ESN output and the EO-EC ground truth, we can conclude that the network learned better the difference between the two conditions in the ADHD population. This advocates for the presence of larger differences in the dynamical regimes of the EEG in the ADHD group than in this of the healthy controls.

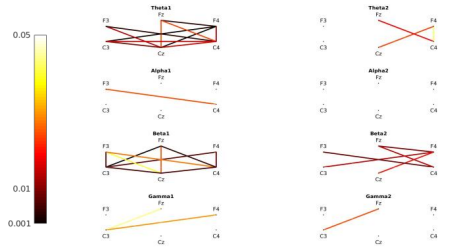

Fig. 4. Connectivity CDSM representation of statistically significant p-values when comparing ADHD and control populations

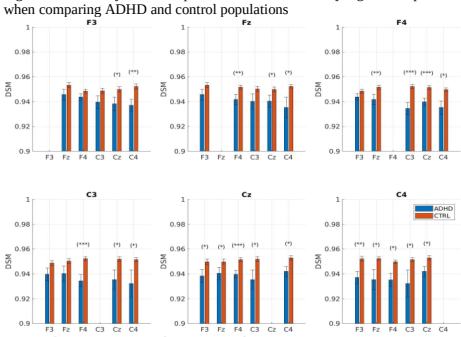

Fig. 5. Theta1 CDSM grand averages and SEM

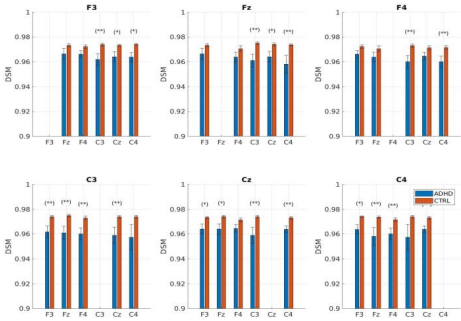

Fig. 6. Beta1 CDSM grand averages and SEM

Figure 7 displays the grand average Dynamical Connectivity Index together with the standard error of the mean. Results are consistent with previously discussed findings. The DCI is smaller in the ADHD population, showing a larger difference in its temporal dynamics between EC-EO conditions. Table II summarizes the statistical significance when comparing the two groups. As can be observed, differences between groups are representative in the theta1, beta1 and beta2 bands.

6

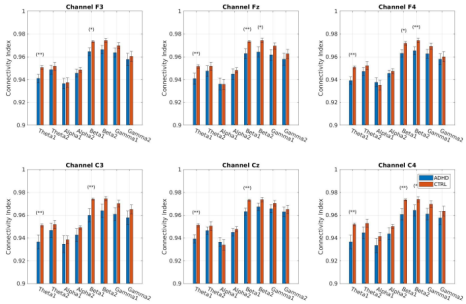

Fig. 7. Dynamical Connectivity Index (DCI) grand averages and standard error of the mean in ADHD and control populations

TABLE II
DYNAMICAL CONNECTIVITY INDEX STATISTICAL SIGNIFICANCE WHEN COMPARING ADHD AND CONTROL POLLUTIONS

	Dynamical Connectivity Index							
	θ_1	θ_2	α_1	α_2	β_1	β_2	γ_1	γ_2
C3	**				*			
Cz	**				**	*	°	
C4	**				*	**		
F3	**				**			
Fz	**				**			
F4	**				**	*		

B. Stationary Band Power Analysis

Figure 8 represents the grand average spectral response together with the standard error of the mean in the 4-45Hz frequency interval. We can observe that the energy in theta and alpha increases in the EC condition for both the ADHD and control groups. When we look independently at each condition we observe an EEG slowing both in EO and EC. This effect is manifested as a shift of the alpha peak frequency towards lower frequencies and an energy increase of low frequency components.

Figure 9 and 10 represent the power grand averages and standard error of the mean for the ADHD and control populations, for both the EO and EC conditions. We observe a power increase in low frequency bands theta and alpha in the ADHD populations for the two conditions. Statistically significant power differences between ADHD and Control groups are presented in Table III and IV, where we can observe that theta2 delivers the most statistically significant differences both for EO and EC conditions.

Figure 11 shows the grand average and standard error of the mean of the EC-EO power ratio metric as defined in section 3.D. In both populations we observe a power increase during EC in low frequencies (theta and alpha), while in high frequencies (beta and gamma) the power increases in EO. Statistical differences between ADHD and control populations were not found at any band or electrode.

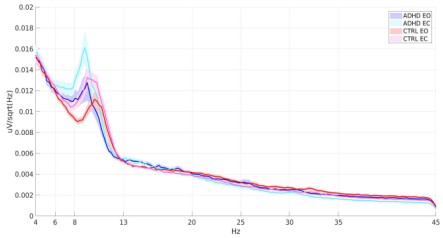

Fig. 8. Grand average spectral response and standard error of the mean of ADHD EO, ADHD EC, Control EO and Control EC populations

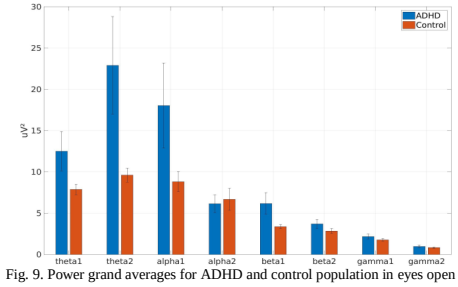

Fig. 9. Power grand averages for ADHD and control population in eyes open

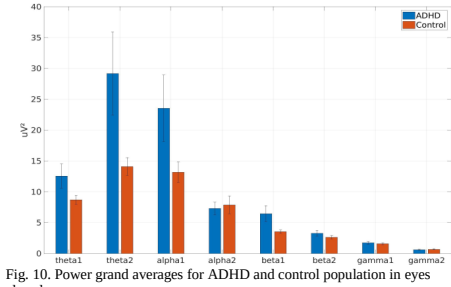

Fig. 10. Power grand averages for ADHD and control population in eyes closed

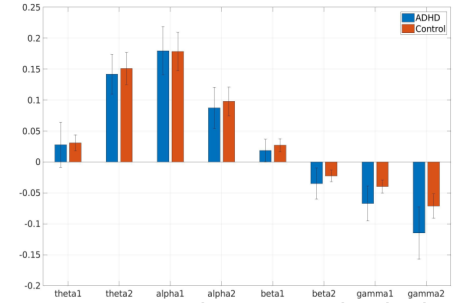

Fig. 11. EC-EO power ratio grand averages in ADHD and control populations

TABLE III

EYES OPEN STATIONARY POWER STATISTICAL SIGNIFICANCE WHEN COMPARING ADHD AND CONTROL POLUATIONS

	Stationary Eyes Closed							
	θ_1	θ_2	α_1	α_2	β_1	β_2	γ_1	γ_2
C3								
Cz		**						
C4								
F3	*	**			*			
Fz	*	**						
F4		**			*			

TABLE IV
EYES CLOSED STATIONARY POWER STATISTICAL SIGNIFICANCE WHEN COMPARING ADHD AND CONTROL POLUATIONS

	Stationary Eyes Open							
	θ_1	θ_2	α_1	α_2	β_1	β_2	γ_1	γ_2
C3		**						
Cz		*						
C4		**						
F3		**			*			
Fz		*						
F4		*			*			

V. DISCUSSION

The diagnostic of ADHD is currently established based on subjective behavioral measures. ADHD diagnosis is therefore biased by cultural, practice and experience factors of clinicians. In the last decades, it has been shown that children suffering from ADHD may have different neural organization, especially in central and frontal areas compared to their age-matched control population. This fact advocates for the use of non-invasive brain monitoring techniques, such as EEG, to quantify abnormal brain activity patterns. Despite great advances in the field of ADHD biomarker discovery, the current state-of-the-art methodologies, such as the well accepted stationary theta increase, beta decrease in ADHDs, have proved insufficiently accurate in many scenarios. Moreover, the non-stationary and chaotic nature of brain activity supports the use of non-stationary techniques capable of detecting abnormal signal dynamics.

ADHD, among other behavioral symptoms, is characterized by a child's inability to sustain attention as well as inappropriate arousal levels. In this study, we propose to study brain activity disparity between low arousal/attention levels (resting eyes closed) and normal attention/arousal levels (resting eyes open) as explained in section 1. Following the ADHD hypoarousal approach our hypothesis relies in that the disparity between these two conditions may be altered in the ADHD population. To measure it we propose a machine-learning based methodology capable of learning dynamical differences between EC-EO conditions. An echo state network input is fed using the filtered temporal series of pairs of electrodes and trained to discriminate between these two. As the amplitude information of these series is removed through standardization, the neural network is believed only to capture the signal dynamics. In previous works we have proved that ESNs are capable of detecting generalized synchronization between two temporal time-series [55]. As we are in a similar scenario we expect ESN to, among other dynamics, detect synchronization variations among channels between EC and EO regimes. The difference between EO and EC has also been studied through a stationary approach that computes the power ratio between EC and EO.

We have analyzed EEG recordings of 21 ADHD children and 30 age-matched controls and studied statistical differences between these two groups. To this effect we have evaluated the performance of stationary power during resting EO and EC, stationary EC-EO power differences and the outcome of the CDSM and DCI features her proposed. Stationary spectral analysis showed an EEG slowing both for EC and EO in the ADHD population, where grand average alpha peak frequency was shifted towards slower frequencies in the ADHD population (Figure 7). A generalized slowing in brain activity can be linked to neurodegenerative and neurodevelopmental disorders and has been largely reported in the ADHD population [58, 59]. Stationary power delivers a statistically significant increase of theta in the ADHD population both in EC and EO conditions (Table III and IV). ADHD children have been largely reported to a show fairly consistent fronto-central theta increase in resting state conditions that has traditionally been associated to a hypo-arousal state [60, 61]. The outcome of this spectral stationary analysis confirms the reliability on the data-set, as two of most reported findings in the literature could be replicated.

The EO-EC stationary power ratio did not deliver statistical differences between the ADHD group and the control population. On the other hand, when analyzing the dynamical variations measured through the hereby proposed Dynamical Connectivity Index, statistically significant differences were found in the theta and beta bands. Abnormalities in these bands have been largely reported in the ADHD population as previously stated in section 1. This study confirms that not only the stationary activity of the brain, but also its temporal dynamics, may be affected at these bands. We have demonstrated that our trained network discriminates better between EC and EO regimes in the ADHD population. This finding indicates an abnormal disparity between low and normal attention/arousal conditions in ADHDs.

Compared to stationary power analysis, the DCI metric here proposed provides larger statistical significance between groups, as observed when comparing results displayed in Table II versus Table III and IV. While DCI provides 11 electrode-band combinations with null hypothesis probability values below 1%, the EO and EC stationary power together provides 8. Whereas these differences were found in theta2 in the stationary power analysis both for EC and EO, DCI provided statistically significant differences below 1% in theta1 and beta1.

Reservoir-computing methodologies, and in particular ESNs, have proved to be an effective technique for EEG feature extraction [39]. Although ESNs have been applied to other EEG analysis scenarios including author's work in Parkinson's disease prognosis [37], this is the first time, to our best knowledge, that it has been used in the ADHD field. The proposed methodology is however not only tied to ADHD

characterization. The here presented approach of measuring the training error of a recurrent neural network used to classify concatenated sequences of different physiological states can be applied to other biomarker discovery modalities. Authors plan in the future to apply this procedure in the field of autism disorder characterization.

VI. Acknowledgements

We specially acknowledge the participants in this study. Funding was provided by the European Commission through the STIPED project under the Horizon 2020 Program (H2020, Grant agreement number 731827). JGO was financially supported by the Spanish Ministry of Economy and Competitiveness and FEDER (project FIS2015-66503-C3-1-P and Maria de Maeztu programme, MDM-2014-0370), the Generalitat de Catalunya (project 2017 SGR 1054), and the ICREA Academia program. We thank Patricia Teruel and Marta García Pérez for their assistance in the EEG recordings.

References

[1] American Psychiatric Association (1994) Diagnostic and statistical manual of mental disorders, 4th ed. American Psychiatric Association, Washington, DC

[2] Cormier, E. (2008). Attention deficit/hyperactivity disorder: a review and update. Journal of pediatric nursing, 23(5), 345-357.

[3] American Psychiatric Association. (2000). Diagnostic criteria from dsM-iV-tr. American Psychiatric Pub.

[4] Rowland, A. S., Lesesne, C. A., & Abramowitz, A. J. (2002). The epidemiology of attention-deficit/hyperactivity disorder (ADHD): a public health view. Mental retardation and developmental disabilities research reviews, 8(3), 162-170.

[5] American Psychiatric Association, 2013

[6] Willcutt, E. G. (2012). The prevalence of DSM-IV attention-deficit/hyperactivity disorder: a meta-analytic review. Neurotherapeutics, 9(3), 490-

[7] Ravens-Sieberer, U., Wille, N., (2008b) Prevalence of mental health problems among children and adolescents in Germany: results of the BELLA study within the National Health Interview and Examination Survey. European child & adolescent psychiatry, 17 Suppl 1, 22-3

[8] American Psychiatric Association. (2013). Diagnostic and statistical manual of mental disorders (5th ed.). Washington, DC: American Psychiatric Association.

[9] Polanczyk, G. V., Willcutt, E. G., Salum, G. A., Kieling, C., & Rohde, L. A. (2014). ADHD prevalence estimates across three decades: an updated systematic review and meta-regression analysis. International Journal of Epidemiology, 43(2), 434-442. doi: 10.1093/ije/dyt261

[10] Crippa, A. et al. (2017). The Utility of a Computerized Algorithm Based on a Multi-Domain Profile of Measures for the Diagnosis of Attention Deficit/Hyperactivity Disorder. Frontiers in Psychiatry, 8 (189). doi: 10.3389/fpsyt.2017.00189

[11] Buyck, I., & Wiersema, J. R. (2014). Resting electroencephalogram in attention deficit hyperactivity disorder: developmental course and diagnostic value. Psychiatry research, 216(3), 391-397

[12] Snyder SM, Rugino TA, Hornig M, Stein MA. Integration of an EEG biomarker with a clinician's ADHD evaluation. Brain Behav. 2015;5: 1–17. doi:10.1002/brb3.330

[13] Geir Ogrim, Juri Kropotov KH. The QEEG theta/beta ratio in ADHD and normal controls: Sensitivity, specificity and behavioral correlates. Psychiatry Res. 2012;198: 482–488. doi:10.1016/j.psychres.2011.12.041

[14] Buyck I, Wiersema JR. Resting electroencephalogram in attention deficit hyperactivity disorder: Developmental course and diagnostic value. Psychiatry Res. 2014;216: 391–397. doi:10.1016/j.psychres.2013.12.055

[15] Clarke AR, Barry RJ, McCarthy R, Selikowitz M, Johnstone SJ, Hsu CI, et al. Coherence in children with Attention-Deficit/Hyperactivity Disorder and excess beta activity in their EEG. Clin Neurophysiol. 2007;118: 1472–1479. doi:10.1016/j.clinph.2007.04.006

[16] Markovska-Simoska, S., & Pop-Jordanova, N. (2017). Quantitative EEG in children and adults with attention deficit hyperactivity disorder: comparison of absolute and relative power spectra and theta/beta ratio. Clinical EEG and neuroscience, 48(1), 20-32.

[17] Gloss, D., Varma, J. K., Pringsheim, T., & Nuwer, M. R. (2016). Practice advisory: The utility of EEG theta/beta power ratio in ADHD diagnosis Report of the Guideline Development, Dissemination, and Implementation Subcommittee of the American Academy of Neurology. Neurology, 87(22), 2375-2379.

[18] Snyder, S. M., Rugino, T. A., Hornig, M., & Stein, M. A. (2015). Integration of an EEG biomarker with a clinician's ADHD evaluation. Brain and behavior, 5(4).

[19] Ogrim, G., Kropotov, J., & Hestad, K. (2012). The quantitative EEG theta/beta ratio in attention deficit/hyperactivity disorder and normal controls: sensitivity, specificity, and behavioral correlates. Psychiatry research, 198(3), 482-488.

[20] Liechti, M. D., Valko, L., Müller, U. C., Döhnert, M., Drechsler, R., Steinhausen, H. C., & Brandeis, D. (2013). Diagnostic value of resting electroencephalogram in attention-deficit/hyperactivity disorder across the lifespan. Brain topography, 26(1), 135-151.

[21] Fabien Lotte. A Tutorial on EEG Signal Processing Techniques for Mental State Recognition in Brain-Computer Interfaces. Eduardo Reck Miranda; Julien Castet. Guide to Brain-Computer Music Interfacing, Springer, 2014.

[22] Coyle, D. (2009). Neural network based auto association and time-series prediction for biosignal processing in brain-computer interfaces. Computational Intelligence Magazine, IEEE, 4(4), 47-59.

[23] Lotte F, Congedo M, Lecuyer A, Lamarche F, Arnaldi B (2007) A review of classification algorithms for EEG-based brain-computer interfaces. Journal of Neural Engineering 4:R1–R13

[24] Lindsley, D. B. (1988). Activation, arousal, alertness, and attention. In States of brain and mind (pp. 1-3). Birkhäuser Boston.

[25] Barbaro, K., Clackson, K., & Wass, S. V. (2017). Infant attention is dynamically modulated with changing arousal levels. Child development, 88(2), 629-639.

[26] Sonuga-Barke EJ, Wiersema JR, van der Meere JJ, Roeyers H (2010) Context-dependent dynamic processes in attention deficit/hyperactivity disorder: differentiating common and unique effects of state regulation deficits and delay aversion. Neuropsychol Rev 20(1):86–102.

[27] Loo, S. K., Hale, T. S., Macion, J., Hanada, G., McGough, J. J., McCracken, J. T., & Smalley, S. L. (2009). Cortical activity patterns in ADHD during arousal, activation and sustained attention. Neuropsychologia, 47(10), 2114-2119.

[28] Geissler, J., Romanos, M., Hegerl, U., & Hensch, T. (2014). Hyperactivity and sensation seeking as autoregulatory attemps to stabilize brain arousal in ADHD and mania? Attention Deficit Hyperactivity Disorder, 6 (159-173). doi: 10.1007/s12402-014-0144-z

[29] Halperin JM, Schulz KP (2006) Revisiting the role of the prefrontal cortex in the pathophysiology of attention-deficit/hyperactivity disorder. Psychol Bull 132(4):560–581

[30] Barry, R. J., & De Blasio, F. M. (2017). EEG Differences between Eyes-Closed and Eyes-Open Resting Remain in Healthy Ageing. Biological Psychology.

[31] Ramachandran, V. S. (2002). Encyclopedia of the Human Brain, Four-Volume Set. Academic Press.

[32] Aminoff, M. J. (2012). Aminoff's Electrodiagnosis in Clinical Neurology E-Book. Elsevier Health Sciences.

[33] Barry, R. J., Clarke, A. R., Johnstone, S. J., Magee, C. A., & Rushby, J. A. (2007). EEG differences between eyes-closed and eyes-open resting conditions. Clinical Neurophysiology, 118(12), 2765-2773.

[34] Coone, A., & Schrauwen, B. (2011). Single trial classification of the P300 evoked potential using Reservoir Computing. In 1st Joint WIC/IEEE SP Symposium on Information Theory and Signal Processing in the Benelux.

[35] Gouy-Pailler, C., Sebag, M., Souloumiac, A., & Larue, A. (2010, August). Ensemble learning for brain computer-interface using uncooperative democratic echo state communities. In Cinquième conférence plénière française de Neurosciences Computationnelles," Neurocomp'10".

[36] Buteneers, P., Verstraeten, D., van Mierlo, P., Wyckhuys, T., Stroobandt, D., Raedt, R., ... & Schrauwen, B. (2011). Automatic detection of epileptic seizures on the intra-cranial electroencephalogram of rats using reservoir computing. Artificial intelligence in medicine, 53(3), 215-223.

[37] Ruffini, G., Ibañez, D., Castellano, M., Dunne, S., & Soria-Frisch, A. (2016, September). EEG-driven RNN classification for prognosis of

neurodegeneration in at-risk patients. In International Conference on Artificial Neural Networks (pp. 306-313). Springer, Cham.
[38] Ayyagari, S. S., Jones, R. D., & Weddell, S. J. (2014, August). EEG-based event detection using optimized echo state networks with leaky integrator neurons. In 2014 36th Annual International Conference of the IEEE Engineering in Medicine and Biology Society (pp. 5856-5859). IEEE
[39] Ibanez-Soria, D., Soria-Frisch A., Garcia-Ojalvo J. Ruffini G. (2018) Echo State Networks Ensemble for SSVEP Dynamical Online Detection, BioRxiv, doi: https://doi.org/10.1101/268581.
[40] Bishop, C. M. (1995). Neural networks for pattern recognition. Oxford university press.
[41] Duda, R. O., Hart, P. E., & Stork, D. G. (2012). Pattern classification. John Wiley & Sons.
[42] Yegnanarayana, B. (2009). Artificial neural networks. PHI Learning Pvt. Ltd.
[43] Schrauwen, B., Verstraeten, D., & Van Campenhout, J. (2007). An overview of reservoir computing: theory, applications and implementations. In Proceedings of the 15th European Symposium on Artificial Neural Networks. p. 471-482 2007 (pp. 471-482).
[44] Jaeger, H.: The "echo state" approach to analysing and training recurrent neural networks. Tech. Rep. GMD Report 148, German National Research Center for Information Technology (2001).
[45] Natschläger, T., Maass, W., & Markram, H. (2002). The" liquid computer": A novel strategy for real-time computing on time series. Special issue on Foundations of Information Processing of TELEMATIK, 8(LNMC-ARTICLE-2002-005), 39-43.
[46] Lukoševičius, M. (2012). A practical guide to applying echo state networks. In Neural networks: Tricks of the trade (pp. 659-686). Springer Berlin Heidelberg
[47] Yildiz, I. B., Jaeger, H., & Kiebel, S. J. (2012). Re-visiting the echo state property. Neural networks, 35, 1-9
[48] David Verstraeten, Joni Dambre, Xavier Dutoit, and Benjamin Schrauwen. Memory versus non-linearity in reservoirs. In Proc. Int Neural Networks (IJCNN) Joint Conf, pages 1–8, 2010.
[49] Fabian Triefenbach, Azarakhsh Jalalvand, Benjamin Schrauwen, and Jean-Pierre Martens. Phoneme recognition with large hierarchical reservoirs. In Advances in Neural Information Processing Systems 23 (NIPS 2010), pages 2307–2315. MIT Press, Cambridge, MA, 201
[50] Wyffels, F., Schrauwen, B., & Stroobandt, D. (2008, September). Stable output feedback in reservoir computing using ridge regression. In International conference on artificial neural networks (pp. 808-817). Springer, Berlin, Heidelberg.
[51] Arns, M., Conners, C. K., & Kraemer, H. C. (2012). A decade of EEG theta/beta ratio research in ADHD: a meta-analysis. Journal of attention disorders, 1087054712460087.
[52] Jurcak, V., Tsuzuki, D., & Dan, I. (2007). 10/20, 10/10, and 10/5 systems revisited: their validity as relative head-surface-based positioning systems. Neuroimage, 34(4), 1600-1611.
[53] Teplan, M. (2002). Fundamentals of EEG measurement. Measurement science review, 2(2), 1-11.
[54] Yegnanarayana, B. (2009). Artificial neural networks. PHI Learning Pvt. Ltd.
[55] Ibáñez-Soria, D., Garcia-Ojalvo, J., Soria-Frisch, A., & Ruffini, G. (2017). Detection of Generalized Synchronization using Echo State Networks. arXiv preprint arXiv:1710.08286.
[56] Bohm, G., & Zech, G. (2010). Introduction to statistics and data analysis for physicists. DESY.
[57] Wilcoxon, F. (1945). Individual comparisons by ranking methods. Biometrics bulletin, 1(6), 80-83.
[58] Vollebregt, M. A., van Dongen-Boomsma, M., Slaats-Willemse, D., Buitelaar, J. K., & Oostenveld, R. (2015). How the individual alpha peak frequency helps unravel the neurophysiologic underpinnings of behavioral functioning in children with attention-deficit/hyperactivity disorder. Clinical EEG and neuroscience, 46(4), 285-291.
[59] Lansbergen, M. M., Arns, M., van Dongen-Boomsma, M., Spronk, D., & Buitelaar, J. K. (2011). The increase in theta/beta ratio on resting-state EEG in boys with attention-deficit/hyperactivity disorder is mediated by slow alpha peak frequency. Progress in Neuro-Psychopharmacology and Biological Psychiatry, 35(1), 47-52
[60] Snyder SM, Hall JR. A meta-analysis of quantitative EEG power associated with attention-deficit hyperactivity disorder. J Clin Neurophysiol. 2006;23:440–455.
[61] Loo, S. K., & Makeig, S. (2012). Clinical utility of EEG in attention-deficit/hyperactivity disorder: a research update. Neurotherapeutics, 9(3), 569-587.

5 Conclusions, Perspectives and Future Work

5.1 Discussion

Nature is dynamic and so is the brain. Therefore, the electrical signals produced by the brain and measured by electroencephalography present non-stationary and chaotic dynamics. Following this rationale, in this Thesis we have successfully employed recurrent neural networks, following the echo-state network (ESN) approach, for feature extraction and classification of EEG signals. We have advanced in the understanding of the detection capabilities of ESNs, demonstrating that ESNs can detect temporal changes in generalized synchronization between two chaotic time-series. We have also used ESNs to characterize the non-stationary dynamics of what is so far considered to be a steady-state phenomenon, SSVEP. Finally, in the field of EEG biomarker discovery, we have successfully proposed a novel non-stationary biomarker for attention deficit hyperactivity disorder. In this section we present and discuss the most relevant findings in each of the studies performed in this Thesis.

5.1.1 Detection of Chaotic Synchronization

Many forms of chaotic synchronization exist including complete, phase, lag and generalized synchronization. In this Thesis we have attempted to analyze the relationships between structural and functional brain regions as a generalized synchronization problem, using ESNs to detect it.

As a first step we have conducted a theoretical study using a chaotic model. Two chaotic Rössler attractors were coupled to construct a series of generalized synchronized sequences interleaved with unsynchronized episodes.

We have demonstrated that ESNs are able to discriminate between time-locked generalized synchronized sequences and unsynchronized ones with great accuracy. The robustness of ESNs for the detection of generalized synchronization in real-world conditions was analyzed by adding noise to the network inputs. ESNs proved to be robust to relatively high levels of noise, supporting the feasibility of their use with real-world data.

Several methodologies for the detection of generalized synchronization exist, including the replica method, the synchronization likelihood, and the mutual false nearest neighbor method [28][29][27]. Compared to them, after their training, ESNs are computationally less costly and can be applied in a continuous manner. This opens the possibility of developing applications based on ESNs capable of monitoring chaotic synchronization changes in real-time. All in all, we have proposed a novel methodology, computationally efficient and with online capabilities for generalized synchronization detection.

5.1.2 Non-Stationary Analysis of Electrophysiological Data Using Echo-State Networks

Stationary methodologies are common in electrophysiology. However, the brain is known to produce high-dimensional non-stationary dynamics, and thus methodologies capable of capturing these patterns are convenient for EEG analysis. In this Thesis we have used ESNs which, as other RNN architectures, incorporate cyclic connections that provide the system with memory and thus with the capability of decoding temporal information. ESNs are capable of detecting neural complexity, non-stationary temporal dynamics, and, as demonstrated in this Thesis, chaotic synchronization between brain sources. We have demonstrated the convenience of non-stationary approaches for feature extraction and detection in two different scenarios. This statement is particularly supported through its comparison with respect to state-of-the-art stationary methodologies.

When ESNs were first introduced in 2001, their novelty was to provide a stable and simple training algorithm at a time when the problem of training RNNs was still not resolved. As of today, with new developments in gradient descend training methods such as Truncated Back Propagation

Through Time (TBPTT), this issue can be considered as sorted out [50]. This fact and the advent of deep learning and other recurrent neural networks architectures such as LSTMs (capable of encoding simultaneously short-and long-term memory) has limited the popularity of ESNs. However, ESNs are still a hot research topic. Their easy training, dynamic capabilities, modularity, distinctive architecture, along with their high performance makes them an ideal RNN choice in multiple scenarios.

In this Thesis we have demonstrated that ESNs are capable of approaching complex problems in the field of EEG data analysis with excellent performance. We have successfully applied ESNs for EEG feature extraction and classification in two different scenarios: 1) in SSVEP characterization and 2) in ADHD biomarker discovery. As in other EEG-based machine learning approaches it has been necessary to implement pre-processing stages that clean and reduce the complexity of EEG signals.

5.1.3 Non-Stationary Characterization of SSVEP Using ESN

Steady-state visual evoked potentials appear as oscillatory components matching the visual flickering frequency and its harmonics when gazing at a repetitive visual stimulation source. This phenomenon is considered to be purely stationary, as explained in Section 1.5. Therefore, state-of-the-art SSVEP detection methods such as PSDA, MSI or CCA exploit this steadiness. Although SSVEP is considered stationary, in this Thesis we have explored non-stationary SSVEP dynamics using ESNs.

We have presented a novel non-stationary SSVEP-detection methodology based on reservoir computing and successfully compared its performance with stationary Canonical Correlation Analysis. To this effect we designed and carried out an experimental campaign in which five participants were stimulated with frequencies ranging from 10 to 22 Hz. Stationary and ESN-based detection delivered dissimilar classifications. For some subjects and frequencies ESN-based methodologies delivered excellent classification accuracy and stationary analysis random detection, while the opposite occurred for other subjects. Our results are consistent with the fact that SSVEP response is a subject, age and stimulation dependent phenomenon.

In particular, we conjecture from our results that these performance discrepancies may reflect the elicitation of evoked responses of a different nature: stationary and non-stationary.

We compared the performance of our proposed ESN-based methodology with the standard CCA approach for different observation windows. The detection capabilities of the ESN-based method proved to be robust with respect to the observation window duration, delivering similar detection accuracy for windows ranging from 0.5 to 4 seconds. On the contrary, in CCA, performance increased with the window length, delivering random classification for 0.5-second windows. This fact favors the communication capabilities of the ESN-based method, which achieves an information transfer rate of 49 bits/minute (with a maximum ITR of 108 bits/minute for one specific subject) compared to the 21 bits/minute rate achieved by the CCA method. Our hypothesis is that the classification capabilities of ESNs may lie in the detection of non-stationary SSVEP dynamics. All things considered, our results validate the application of ESNs in SSVEP-based applications.

5.1.4 ESN-Based ADHD Biomarker

Attention-Deficit Hyperactivity Disorder (ADHD), introduced in Section 1.5, is one of the most common neurodevelopmental and psychiatric disorders of childhood. ADHD diagnosis is based on interviews and behavioral observation. Thus ADHD diagnosis is subjective and depends heavily on the experience and practical knowledge of clinicians. Likewise, medication shows serious side effects and is generally applied in a trial and error manner. Reliable markers that support ADHD diagnosis are thus necessary.

Given its non-invasiveness, cost-effectiveness and brain monitoring capabilities, EEG has been used for decades in ADHD characterization. In this Thesis we propose a novel non-stationary ADHD biomarker inspired in the hypoarousal ADHD theory. This theory states that ADHD children show arousal deficits and try to compensate them by way of self-stimulation through excessive activity. We propose a novel approach that quantifies

EEG differences between two conditions: 1) low arousal state (resting eyes-closed) and 2) normal arousal states (resting eyes-open). We successfully validated the hypothesis that differences between the two conditions are abnormal in the ADHD population.

The new methodology proposed here, based on ESNs, is capable of quantifying non-stationary differences and synchronization changes between the eyes-closed and eyes-open conditions within pairs of electrodes. These differences are measured at specific brain rhythms. Our results show that the ADHD population (N=21) has larger differences between conditions than its age-matched control (N=31) population. These differences are statistically significant between groups in the theta and beta bands. Interestingly these are the same bands of largely reported alterations in band power, suggesting that both stationary and non-stationary dynamics within these bands may be altered in the ADHD population. Differences between the eyes-closed and eyes-open conditions were also assessed using stationary band power approaches. In this case no statistical significance between groups was found in the study populations. The statistical significance of the proposed non-stationary feature was larger than state-of-the-art band-power approaches, highlighting its applicability for the characterization of ADHD.

In summary, our results reveal a new robust feature of ADHD that can be used to quantify changes in the non-stationary dynamics between low- and normal-arousal conditions. This is the first time, to the best of our knowledge, that ESNs are used for ADHD characterization.

5.2 Summary of Achievements

- We have demonstrated that ESNs are capable of detecting changes in generalized synchronization between two chaotic time series.
- We have validated the applicability of ESNs to EEG analysis in two different scenarios, in both at the therapeutic (BCI) and diagnostic (ADHD) applications.
- ESNs have been applied for the first time to SSVEP characterization.

- Based on the obtained results, we have made the hypothesis that, in addition to its well known steady-state response, SSVEP may possess non-stationary features.
- A novel methodology for SSVEP detection based on an ensemble of ESNs has been proposed. The proposed approach outperformed state-of-the-art stationary methodologies in terms of information transfer rate.
- We have applied ESNs for the first time to ADHD characterization.
- We have successfully proposed a novel ADHD biomarker based on ESNs, capable of quantifying non-stationary changes between low and normal arousal conditions.

5.3 Perspective and Future Work

5.3.1 ESN Chaotic Synchronization Detection Capabilities

Echo-state networks have proven to be capable of detecting generalized synchronization changes between two temporal series. This demonstrates their ability to detect chaotic synchronization. Synchronization presents a variety of forms depending on the nature of the interacting systems. Many types of chaotic synchronization exist, among them lag, phase and amplitude envelope synchronization. The synchronization detection capabilities of ESNs should be further explored for these and other forms of synchronization between coupled dynamical systems.

5.3.2 Generalized Synchronization Detection Validation Using Experimental Data

In this Thesis two Rössler attractors have being numerically simulated. These attractors are coupled and de-coupled in order to simulate generalized synchronized time sequences, followed by unsynchronized ones. Real environments have been simulated through the addition of Gaussian noise of different amplitude levels to these attractors, as a first stage to validate real-world feasibility. It is possible to construct driver and driven attractors using electronic circuits and coupled them in a generalized synchronized

way [146]. Using the data obtained by digitally collecting the outcome of these circuits, the capabilities of ESNs for the detection of generalized synchronization can be tested in experimental data.

5.3.3 Comparison with Other Generalized Synchronization Detection Approaches

Several methodologies exist for the detection of generalized synchronization. In order to gain a better understanding of the capabilities of ESNs, its detection performance and computational cost, among others, can be compared with respect to state-of-the-art generalized synchronization detection methodologies. This comparison may be of special interest in noisy environments that simulate their applicability in real world scenarios.

5.3.4 Non-Stationary Nature of the SSVEP

Based on our results, our hypothesis is that apart from the largely reported steady-state resonance effect, the neural response to repetitive visual stimulation may possess any non-stationary properties. However the type of dynamics this form of stimulation may elicit remains unknown. Signal complexity, chaotic patterns and different forms of synchronization should be studied in order to gain a better understanding of the underlying processes elicited by repetitive visual stimulation. The study of these dynamics would be of special interest for the fields of cognitive and clinical neuroscience.

5.3.5 Hybrid Stationary/Non-Stationary BCI Approach

In this Thesis we have proposed a novel SSVEP extraction and classification methodology based on an ensemble of ESNs. The proposed methodology outperforms state-of-the-art canonical correlation analysis (CCA) in terms of detection accuracy and information transfer rate when a BCI system with 6 degrees of freedom is simulated. Results suggest that methodologies (ESN and CCA) are capturing different features of the SSVEP response, and are thus complementary. It would be interesting to validate the efficacy of the ESN-based detection method using a larger experimental

data-set. Additionally, the construction of a BCI system capable of quantifying both the stationary and non-stationary dynamics of SSVEP response may deliver a better detection performance.

5.3.6 ADHD Biomarker Validation

Compared to other ADHD studies, the experimental data-set used here, consisting of 51 children with ages ranging from 7 to 11 years old, is considered adequate to demonstrate the validity of the novel ADHD feature proposed in this Thesis. Nevertheless, further studies should confirm its efficacy using different, and in particular larger, data-sets. ADHD is a very heterogeneous disorder, with three main symptoms-based sub-types: inattentive, hyperactive and combined, as presented in Section 1.5. The ESN-based approach presented here can be applied to age, gender or ADHD type stratified data. This may serve to gain a better understanding of the abnormal EEG dynamics in ADHD children and improve statistical significance between ADHD and the control group. We plan to carry out this validation within the Horizon 2020 EU project STIPED (Grant agreement number 731827), which aims to study non-invasive brain stimulation in pediatric neuro-psychiatric disorders.

5.3.7 Decision Support System for ADHD Diagnosis

We can also envision the feasibility of designing a decision-support system using the ESN-based biomarker proposed here. This system would support clinicians in establishing the ADHD diagnosis. Its performance could be compared to NEBA, introduced in Section 1.5.4., which is so far the only FDA approved EEG-based method to assist in ADHD diagnosis.

5.3.8 Application to Other Neurodevelopmental Disorders

The ADHD feature presented here is based in quantifying non-stationary differences between two cognitive states, in this case resting eyes-open and eyes-closed conditions. This methodology could be used in other biomarker-discovery scenarios with the same cognitive states, or other higher demanding mental tasks. We plan to apply this procedure in the near future to the field of autism disorder biomarker discovery also within STIPED project.

Bibliography

[1] B. Widrow and M. E. Hoff, "Adaptive switching circuits", STANFORD UNIV CA STANFORD ELECTRONICS LABS, Tech. Rep., 1960.

[2] B. Widrow and M. A. Lehr, "30 years of adaptive neural networks: Perceptron, madaline, and backpropagation", *Proceedings of the IEEE*, vol. 78, no. 9, pp. 1415–1442, 1990.

[3] J. I. Glaser, A. S. Benjamin, R. Farhoodi, and K. P. Kording, "The roles of supervised machine learning in systems neuroscience", *ArXiv preprint arXiv:1805.08239*, 2018.

[4] T. C. Kietzmann, P. McClure, and N. Kriegeskorte, "Deep neural networks in computational neuroscience", *BioRxiv*, p. 133 504, 2017.

[5] T. McKenna, T. McMullen, and M. Shlesinger, "The brain as a dynamic physical system", *Neuroscience*, vol. 60, no. 3, pp. 587–605, 1994.

[6] H. Jaeger, "The echo state approach to analysing and training recurrent neural networks-with an erratum note", *Bonn, Germany: German National Research Center for Information Technology GMD Technical Report*, vol. 148, no. 34, p. 13, 2001.

[7] L. Appeltant, M. C. Soriano, G. Van der Sande, J. Danckaert, S. Massar, J. Dambre, B. Schrauwen, C. R. Mirasso, and I. Fischer, "Information processing using a single dynamical node as complex system", *Nature communications*, vol. 2, p. 468, 2011.

[8] L. Larger, M. C. Soriano, D. Brunner, L. Appeltant, J. M. Gutiérrez, L. Pesquera, C. R. Mirasso, and I. Fischer, "Photonic information processing beyond turing: An optoelectronic implementation of reservoir computing", *Optics express*, vol. 20, no. 3, pp. 3241–3249, 2012.

[9] D. Kudithipudi, Q. Saleh, C. Merkel, J. Thesing, and B. Wysocki, "Design and analysis of a neuromemristive reservoir computing architecture for biosignal processing", *Frontiers in neuroscience*, vol. 9, p. 502, 2016.

[10] M. I. Rabinovich, K. J. Friston, and P. Varona, *Principles of brain dynamics: Global state interactions*. MIT Press, 2012.

[11] J. P. Pijn, J. Van Neerven, A. Noest, and F. H. L. da Silva, "Chaos or noise in eeg signals; dependence on state and brain site", *Electroencephalography and clinical Neurophysiology*, vol. 79, no. 5, pp. 371–381, 1991.

[12] A Krakovska *et al.*, "Two decades of search for chaos in brain", *MEASUREMENT*, pp. 90–94, 2009.

[13] W. s. Pritchard and D. w. Duke, "Measuring chaos in the brain: A tutorial review of nonlinear dynamical eeg analysis", *International Journal of Neuroscience*, vol. 67, no. 1-4, pp. 31–80, 1992.

[14] C. A. Skarda and W. J. Freeman, "How brains make chaos in order to make sense of the world", *Behavioral and brain sciences*, vol. 10, no. 2, pp. 161–173, 1987.

[15] L. Medsker and L. Jain, "Recurrent neural networks", *Design and Applications*, vol. 5, 2001.

[16] A. V. Oppenheim, R. W. Schafer, and C. Yuen, "Digital signal processing", *IEEE Transactions on Systems, Man, and Cybernetics*, vol. 8, no. 2, pp. 146–146, 1978.

[17] T. W. Anderson, *The statistical analysis of time series*. John Wiley & Sons, 2011, vol. 19.

[18] M. B. Priestley, "Non-linear and non-stationary time series analysis", 1988.

[19] A. Soria-Frisch, *Soft data fusion for computer vision*. Fraunhofer-IRB-Verlag, 2004.

[20] S. Wiggins, *Introduction to applied nonlinear dynamical systems and chaos*. Springer Science & Business Media, 2003, vol. 2.

[21] C. Webber, "Recurrence quantification of fractal structures", *Frontiers in physiology*, vol. 3, p. 382, 2012.

[22] S. Boccaletti, J. Kurths, G. Osipov, D. Valladares, and C. Zhou, "The synchronization of chaotic systems", *Physics reports*, vol. 366, no. 1-2, pp. 1–101, 2002.

[23] H. Fujisaka and T. Yamada, "Stability theory of synchronized motion in coupled-oscillator systems", *Progress of theoretical physics*, vol. 69, no. 1, pp. 32–47, 1983.

[24] M. G. Rosenblum, A. S. Pikovsky, and J. Kurths, "Phase synchronization of chaotic oscillators", *Physical review letters*, vol. 76, no. 11, p. 1804, 1996.

[25] M. G. Rosenblum, A. S. Pikovsky, and J. Kurths, "From phase to lag synchronization in coupled chaotic oscillators", *Physical Review Letters*, vol. 78, no. 22, p. 4193, 1997.

[26] R. Femat and G. Solis-Perales, "On the chaos synchronization phenomena", *Physics Letters A*, vol. 262, no. 1, pp. 50–60, 1999.

[27] N. F. Rulkov, M. M. Sushchik, L. S. Tsimring, and H. D. Abarbanel, "Generalized synchronization of chaos in directionally coupled chaotic systems", *Physical Review E*, vol. 51, no. 2, p. 980, 1995.

[28] C. Stam and B. Van Dijk, "Synchronization likelihood: An unbiased measure of generalized synchronization in multivariate data sets", *Physica D: Nonlinear Phenomena*, vol. 163, no. 3-4, pp. 236–251, 2002.

[29] H. D. Abarbanel, N. F. Rulkov, and M. M. Sushchik, "Generalized synchronization of chaos: The auxiliary system approach", *Physical Review E*, vol. 53, no. 5, p. 4528, 1996.

[30] T. M. Mitchell, *The discipline of machine learning*. Carnegie Mellon University, School of Computer Science, Machine Learning Department, 2006, vol. 9.

[31] C. Bishop, C. M. Bishop, *et al.*, *Neural networks for pattern recognition*. Oxford university press, 1995.

[32] I. A. Basheer and M Hajmeer, "Artificial neural networks: Fundamentals, computing, design, and application", *Journal of microbiological methods*, vol. 43, no. 1, pp. 3–31, 2000.

[33] W. Waldeyer, "Ueber einige neuere forschungen im gebiete der anatomie des centralnervensystems1", *DMW-Deutsche Medizinische Wochenschrift*, vol. 17, no. 44, pp. 1213–1218, 1891.

[34] E. Tansey, "Not committing barbarisms: Sherrington and the synapse, 1897", *Brain research bulletin*, vol. 44, no. 3, pp. 211–212, 1997.

[35] G. M. Shepherd, *The synaptic organization of the brain*. Oxford University Press, 2003.

[36] F. Rosenblatt, "The perceptron: A probabilistic model for information storage and organization in the brain.", *Psychological review*, vol. 65, no. 6, p. 386, 1958.

[37] F. Rosenblatt, "Principles of neurodynamics. perceptrons and the theory of brain mechanisms", CORNELL AERONAUTICAL LAB INC BUFFALO NY, Tech. Rep., 1961.

[38] D. E. Rumelhart, J. L. McClelland, P. R. Group, *et al.*, *Parallel distributed processing*. MIT press Cambridge, MA, 1987, vol. 1.

[39] G. V. Puskorius, L. A. Feldkamp, and L. I. Davis, "Dynamic neural network methods applied to on-vehicle idle speed control", *Proceedings of the IEEE*, vol. 84, no. 10, pp. 1407–1420, 1996.

[40] Z. C. Lipton, J. Berkowitz, and C. Elkan, "A critical review of recurrent neural networks for sequence learning", *ArXiv preprint: 1506.00019*, 2015.

[41] S. Haykin and N. Network, "A comprehensive foundation", *Neural networks*, vol. 2, no. 2004, p. 41, 2004.

[42] J. F. Kolen and S. C. Kremer, *A field guide to dynamical recurrent networks*. John Wiley & Sons, 2001.

[43] R. J. Williams and D. Zipser, "A learning algorithm for continually running fully recurrent neural networks", *Neural computation*, vol. 1, no. 2, pp. 270–280, 1989.

[44] S. Hochreiter and J. Schmidhuber, "Long short-term memory", *Neural computation*, vol. 9, no. 8, pp. 1735–1780, 1997.

[45] W. Maass, T. Natschläger, and H. Markram, "Real-time computing without stable states: A new framework for neural computation based on perturbations", *Neural computation*, vol. 14, no. 11, pp. 2531–2560, 2002.

[46] D. Verstraeten, B. Schrauwen, M. d Haene, and D. Stroobandt, "An experimental unification of reservoir computing methods", *Neural networks*, vol. 20, no. 3, pp. 391–403, 2007.

[47] J. J. Steil, "Backpropagation-decorrelation: Online recurrent learning with o (n) complexity", in *Neural Networks, 2004. Proceedings. 2004 IEEE International Joint Conference on*, IEEE, vol. 2, 2004, pp. 843–848.

[48] J ürgen Schmidhuber, D. Wierstra, M. Gagliolo, and F. Gomez, "Training recurrent networks by evolino",

[49] H. Jaeger, "Adaptive nonlinear system identification with echo state networks", in *Advances in neural information processing systems*, 2003, pp. 609–616.

[50] H. Jaeger, "Echo state network", *Scholarpedia*, vol. 2, no. 9, p. 2330, 2007.

[51] I. B. Yildiz, H. Jaeger, and S. J. Kiebel, "Re-visiting the echo state property", *Neural networks*, vol. 35, pp. 1–9, 2012.

[52] G. Manjunath and H. Jaeger, "Echo state property linked to an input: Exploring a fundamental characteristic of recurrent neural networks", *Neural computation*, vol. 25, no. 3, pp. 671–696, 2013.

[53] M. Lukoševičius and H. Jaeger, "Reservoir computing approaches to recurrent neural network training", *Computer Science Review*, vol. 3, no. 3, pp. 127–149, 2009.

[54] D. Verstraeten, J. Dambre, X. Dutoit, and B. Schrauwen, "Memory versus non linearity in reservoirs", in *Neural Networks (IJCNN), The 2010 International Joint Conference on*, IEEE, 2010, pp. 1–8.

[55] H. Jaeger, *Tutorial on training recurrent neural networks, covering BPPT, RTRL, EKF and the" echo state network" approach*. GMD Forschungszentrum Informationstechnik Bonn, 2002, vol. 5.

[56] A. E. Hoerl and R. W. Kennard, "Ridge regression: Biased estimation for nonorthogonal problems", *Technometrics*, vol. 12, no. 1, pp. 55–67, 1970.

[57] F. Wyffels, B. Schrauwen, and D. Stroobandt, "Stable output feedback in reservoir computing using ridge regression", in *International conference on artificial neural networks*, Springer, 2008, pp. 808–817.

[58] M. Lukoševičius, "A practical guide to applying echo state networks", in *Neural networks: Tricks of the trade*, Springer, 2012, pp. 659–686.

[59] E. Niedermeyer and F. L. da Silva, *Electroencephalography: Basic principles, clinical applications, and related fields*. Lippincott Williams & Wilkins, 2005.

[60] G. Buzsaki, *Rhythms of the Brain*. Oxford University Press, 2006.

[61] F. L. da Silva, "Eeg and meg: Relevance to neuroscience", *Neuron*, vol. 80, no. 5, pp. 1112–1128, 2013.

[62] D. O. Hebb, *The organization of behavior: A neuropsychological theory*. Psychology Press, 2005.

[63] A. D. Legatt, J. Arezzo, and H. G. Vaughan Jr, "Averaged multiple unit activity as an estimate of phasic changes in local neuronal activity: Effects of volume-conducted potentials", *Journal of neuroscience methods*, vol. 2, no. 2, pp. 203–217, 1980.

[64] S. Murakami and Y. Okada, "Contributions of principal neocortical neurons to magnetoencephalography and electroencephalography signals", *The Journal of physiology*, vol. 575, no. 3, pp. 925–936, 2006.

[65] R. K. Mehta and R. Parasuraman, "Neuroergonomics: A review of applications to physical and cognitive work", *Frontiers in human neuroscience*, vol. 7, p. 889, 2013.

[66] H. Berger, "Über das elektrenkephalogramm des menschen", *Archiv für psychiatrie und nervenkrankheiten*, vol. 87, no. 1, pp. 527–570, 1929.

[67] W. O. Tatum IV, *Handbook of EEG interpretation*. Demos Medical Publishing, 2014.

[68] G. Thut, C. Miniussi, and J. Gross, "The functional importance of rhythmic activity in the brain", *Current Biology*, vol. 22, no. 16, R658–R663, 2012.

[69] A. Riera Sardà, "Computational intelligence techniques for electrophysiological data analysis", 2012.

[70] T. J. Sejnowski and O. Paulsen, "Network oscillations: Emerging computational principles", *Journal of Neuroscience*, vol. 26, no. 6, pp. 1673–1676, 2006.

[71] S. J. Van Albada and P. A. Robinson, "Relationships between electroencephalographic spectral peaks across frequency bands", *Frontiers in human neuroscience*, vol. 7, p. 56, 2013.

[72] N. Bigdely-Shamlo, T. Mullen, C. Kothe, K.-M. Su, and K. A. Robbins, "The prep pipeline: Standardized preprocessing for large-scale eeg analysis", *Frontiers in neuroinformatics*, vol. 9, p. 16, 2015.

[73] X. Lei and K. Liao, "Understanding the influences of eeg reference: A large-scale brain network perspective", *Frontiers in neuroscience*, vol. 11, p. 205, 2017.

[74] M. Teplan *et al.*, "Fundamentals of eeg measurement", *Measurement science review*, vol. 2, no. 2, pp. 1–11, 2002.

[75] B. A. Cohen and A. Sances, "Stationarity of the human electroencephalogram", *Medical and Biological Engineering and Computing*, vol. 15, no. 5, pp. 513–518, 1977.

[76] C. Bugli and P. Lambert, "Comparison between principal component analysis and independent component analysis in electroencephalograms modelling", *Biometrical Journal*, vol. 49, no. 2, pp. 312–327, 2007.

[77] S. Luck, "An introduction to the event-related potential technique. 2005", *Massachusetts: The MIT Press Google Scholar*,

[78] E. O. Brigham and E. O. Brigham, *The fast Fourier transform and its applications*. prentice Hall Englewood Cliffs, NJ, 1988, vol. 1.

[79] P. Welch, "The use of fast fourier transform for the estimation of power spectra: A method based on time averaging over short, modified periodograms", *IEEE Transactions on audio and electroacoustics*, vol. 15, no. 2, pp. 70–73, 1967.

[80] M. Akin, "Comparison of wavelet transform and fft methods in the analysis of eeg signals", *Journal of medical systems*, vol. 26, no. 3, pp. 241–247, 2002.

[81] M. X. Cohen, *Analyzing neural time series data: Theory and practice*. MIT press, 2014.

[82] C. J. Stam, G. Nolte, and A. Daffertshofer, "Phase lag index: Assessment of functional connectivity from multi channel eeg and meg with diminished bias from common sources", *Human brain mapping*, vol. 28, no. 11, pp. 1178–1193, 2007.

[83] G. Dornhege, *Toward brain-computer interfacing*. MIT press, 2007.

[84] F. B. Vialatte, J. Dauwels, M. Maurice, Y. Yamaguchi, and A. Cichocki, "On the synchrony of steady state visual evoked potentials and oscillatory burst events", *Cognitive neurodynamics*, vol. 3, no. 3, pp. 251–261, 2009.

[85] T. Tsoneva, G. Garcia-Molina, and P. Desain, "Neural dynamics during repetitive visual stimulation", *Journal of neural engineering*, vol. 12, no. 6, p. 066 017, 2015.

[86] A. Birca, L. Carmant, A. Lortie, P. Vannasing, H. Sauerwein, M. Robert, L. Lemay, X.-P. Wang, D. Piper, V. Donici, *et al.*, "Maturational changes of 5 hz ssveps elicited by intermittent photic stimulation", *International Journal of Psychophysiology*, vol. 78, no. 3, pp. 295–298, 2010.

[87] R. Srinivasan, F. A. Bibi, and P. L. Nunez, "Steady-state visual evoked potentials: Distributed local sources and wave-like dynamics are sensitive to flicker frequency", *Brain topography*, vol. 18, no. 3, pp. 167–187, 2006.

[88] D. Zhu, J. Bieger, G. G. Molina, and R. M. Aarts, "A survey of stimulation methods used in ssvep-based bcis", *Computational intelligence and neuroscience*, vol. 2010, p. 1, 2010.

[89] F. Wan, J. N. Da Cruz, W. Nan, C. M. Wong, M. I. Vai, and A. Rosa, "Alpha neurofeedback training improves ssvep-based bci performance", *Journal of neural engineering*, vol. 13, no. 3, p. 036 019, 2016.

[90] R. Ossmann, D. Thaller, G. Nussbaum, F. Pühretmair, C. Veigl, C. Weiß, B. Morales, and U. Diaz, "Asterics, a flexible assistive technology construction set", *Procedia Computer Science*, vol. 14, pp. 1–9, 2012.

[91] C. Veigl, C. Weiß, K. Kakousis, D. Ibáñez, A. Soria-Frisch, and A. Carbone, "Model-based design of novel human-computer interfaces, the assistive technology rapid integration & construction set (asterics)", in *Biosignals and Biorobotics Conference (BRC), 2013 ISSNIP*, IEEE, 2013, pp. 1–7.

[92] S Sheykhivand, T. Y. Rezaii, A. N. Saatlo, and N Romooz, "Comparison between different methods of feature extraction in bci systems based on ssvep", *International Journal of Industrial Mathematics*, vol. 9, p. 1, 2017.

[93] V. P. Oikonomou, G. Liaros, K. Georgiadis, E. Chatzilari, K. Adam, S. Nikolopoulos, and I. Kompatsiaris, "Comparative evaluation of state-of-the-art algorithms for ssvep-based bcis", *ArXiv:1602.00904*, 2016.

[94] R. M. Tello, S. M. Muller, T. Bastos-Filho, and A. Ferreira, "A comparison of techniques and technologies for ssvep classification", in *Biosignals and Biorobotics Conference (2014): Biosignals and Robotics for Better and Safer Living (BRC), 5th ISSNIP-IEEE*, IEEE, 2014, pp. 1–6.

[95] S. M. T. Müller, T. F. Bastos-Filho, and M. Sarcinelli-Filho, "Incremental ssvep analysis for bci implementation", in *Engineering in Medicine and Biology Society (EMBC), 2010 Annual International Conference of the IEEE*, IEEE, 2010, pp. 3333–3336.

[96] Z. Lin, C. Zhang, W. Wu, and X. Gao, "Frequency recognition based on canonical correlation analysis for ssvep-based bcis", *IEEE transactions on biomedical engineering*, vol. 53, no. 12, pp. 2610–2614, 2006.

[97] X. Chen, Y. Wang, S. Gao, T.-P. Jung, and X. Gao, "Filter bank canonical correlation analysis for implementing a high-speed ssvep-based brain–computer interface", *Journal of neural engineering*, vol. 12, no. 4, p. 046 008, 2015.

[98] Y. Zhang, P. Xu, K. Cheng, and D. Yao, "Multivariate synchronization index for frequency recognition of ssvep-based brain–computer interface", *Journal of neuroscience methods*, vol. 221, pp. 32–40, 2014.

[99] Y. Zhang, J. Jin, X. Qing, B. Wang, and X. Wang, "Lasso based stimulus frequency recognition model for ssvep bcis", *Biomedical Signal Processing and Control*, vol. 7, no. 2, pp. 104–111, 2012.

[100] S. Ge, R. Wang, Y. Leng, H. Wang, P. Lin, and K. Iramina, "A double-partial least-squares model for the detection of steady-state visual evoked potentials", *IEEE Journal of Biomedical and Health informatics*, vol. 21, no. 4, pp. 897–903, 2017.

[101] F.-B. Vialatte, M. Maurice, J. Dauwels, and A. Cichocki, "Steady-state visually evoked potentials: Focus on essential paradigms and future perspectives", *Progress in neurobiology*, vol. 90, no. 4, pp. 418–438, 2010.

[102] J. R. Wolpaw, N. Birbaumer, W. J. Heetderks, D. J. McFarland, P. H. Peckham, G. Schalk, E. Donchin, L. A. Quatrano, C. J. Robinson, T. M. Vaughan, *et al.*, "Brain-computer interface technology: A review of the first international meeting", *IEEE transactions on rehabilitation engineering*, vol. 8, no. 2, pp. 164–173, 2000.

[103] M. Cheng, X. Gao, S. Gao, and D. Xu, "Design and implementation of a brain-computer interface with high transfer rates", *IEEE transactions on biomedical engineering*, vol. 49, no. 10, pp. 1181–1186, 2002.

[104] M. M. Müller and S. Hillyard, "Concurrent recording of steady-state and transient event-related potentials as indices of visual-spatial selective attention", *Clinical Neurophysiology*, vol. 111, no. 9, pp. 1544–1552, 2000.

[105] S. Morgan, J. Hansen, and S. Hillyard, "Selective attention to stimulus location modulates the steady-state visual evoked potential", *Proceedings of the National Academy of Sciences*, vol. 93, no. 10, pp. 4770–4774, 1996.

[106] M. M. Müller, T. W. Picton, P. Valdes-Sosa, J. Riera, W. A. Teder-Sälejärvi, and S. A. Hillyard, "Effects of spatial selective attention on the steady-state visual evoked potential in the 20–28 hz range", *Cognitive Brain Research*, vol. 6, no. 4, pp. 249–261, 1998.

[107] C.-M. Giabbiconi, V. Jurilj, T. Gruber, and S. Vocks, "Steady-state visually evoked potential correlates of human body perception", *Experimental brain research*, vol. 234, no. 11, pp. 3133–3143, 2016.

[108] M. J. Wieser, V. Miskovic, and A. Keil, "Steady-state visual evoked potentials as a research tool in social affective neuroscience", *Psychophysiology*, vol. 53, no. 12, pp. 1763–1775, 2016.

[109] R. B. Silberstein, P. L. Nunez, A. Pipingas, P. Harris, and F. Danieli, "Steady state visually evoked potential (ssvep) topography in a graded working memory task", *International Journal of Psychophysiology*, vol. 42, no. 2, pp. 219–232, 2001.

[110] H. N. Macpherson, D. J. White, K. A. Ellis, C. Stough, D. Camfield, R. Silberstein, and A. Pipingas, "Age-related changes to the neural correlates of working memory which emerge after midlife", *Frontiers in aging neuroscience*, vol. 6, p. 70, 2014.

[111] A. Horwitz, M. D. Thomsen, I. Wiegand, H. Horwitz, M. Klemp, M. Nikolic, L. Rask, M. Lauritzen, and K. Benedek, "Visual steady state in relation to age and cognitive function", *PloS one*, vol. 12, no. 2, e0171859, 2017.

[112] F. Pei, S. Baldassi, and A. M. Norcia, "Electrophysiological measures of low-level vision reveal spatial processing deficits and hemispheric asymmetry in autism spectrum disorder", *Journal of vision*, vol. 14, no. 11, pp. 3–3, 2014.

[113] A. Dickinson, R. Gomez, M. Jones, V. Zemon, and E. Milne, "Lateral inhibition in the autism spectrum: An ssvep study of visual cortical lateral interactions", *Neuropsychologia*, vol. 111, pp. 369–376, 2018.

[114] P. D. Butler and D. C. Javitt, "Early-stage visual processing deficits in schizophrenia", *Current opinion in psychiatry*, vol. 18, no. 2, p. 151, 2005.

[115] A. Lenartowicz and S. K. Loo, "Use of eeg to diagnose adhd", *Current psychiatry reports*, vol. 16, no. 11, p. 498, 2014.

[116] E. Cormier, "Attention deficit/hyperactivity disorder: A review and update", *Journal of pediatric nursing*, vol. 23, no. 5, pp. 345–357, 2008.

[117] A. Diagnostic, *Statistical manual of mental disorders dsm-iv-tr, american psychiatric association task force on dsm-iv*, 2000.

[118] A. P. Association *et al.*, *Diagnostic and statistical manual of mental disorders (DSM-5®)*. American Psychiatric Pub, 2013.

[119] E. G. Willcutt, "The prevalence of dsm-iv attention-deficit hyperactivity disorder: A meta-analytic review", *Neurotherapeutics*, vol. 9, no. 3, pp. 490–499, 2012.

[120] W. H. Organization, *International statistical classification of diseases and related health problems*. World Health Organization, 2004, vol. 1.

[121] J. D. Kropotov, *Functional neuromarkers for psychiatry: Applications for diagnosis and treatment*. Academic Press, 2016.

[122] K. Bruchmüller, J. Margraf, and S. Schneider, "Is adhd diagnosed in accord with diagnostic criteria? overdiagnosis and influence of client gender on diagnosis.", *Journal of consulting and clinical psychology*, vol. 80, no. 1, p. 128, 2012.

[123] E. C. Merten, J. C. Cwik, J. Margraf, and S. Schneider, "Overdiagnosis of mental disorders in children and adolescents (in developed countries)", *Child and adolescent psychiatry and mental health*, vol. 11, no. 1, p. 5, 2017.

[124] A. Crippa, C. Salvatore, E. Molteni, M. Mauri, A. Salandi, S. Trabattoni, C. Agostoni, M. Molteni, M. Nobile, and I. Castiglioni, "The utility of a computerized algorithm based on a multi-domain profile of measures for the diagnosis of attention deficit/hyperactivity disorder", *Frontiers in Psychiatry*, vol. 8, p. 189, 2017.

[125] J. Geissler, M. Romanos, U. Hegerl, and T. Hensch, "Hyperactivity and sensation seeking as autoregulatory attempts to stabilize brain arousal in adhd and mania?", *ADHD Attention Deficit and Hyperactivity Disorders*, vol. 6, no. 3, pp. 159–173, 2014.

[126] J. M. Halperin and K. P. Schulz, "Revisiting the role of the prefrontal cortex in the pathophysiology of attention-deficit/hyperactivity disorder.", *Psychological bulletin*, vol. 132, no. 4, p. 560, 2006.

[127] S. Sikström and G. Söderlund, "Stimulus-dependent dopamine release in attention-deficit/hyperactivity disorder.", *Psychological review*, vol. 114, no. 4, p. 1047, 2007.

[128] J. Sergeant, "The cognitive-energetic model: An empirical approach to attention-deficit hyperactivity disorder", *Neuroscience & Biobehavioral Reviews*, vol. 24, no. 1, pp. 7–12, 2000.

[129] K. W. Lange, S. Reichl, K. M. Lange, L. Tucha, and O. Tucha, "The history of attention deficit hyperactivity disorder", *ADHD Attention Deficit and Hyperactivity Disorders*, vol. 2, no. 4, pp. 241–255, 2010.

[130] L. Thompson and M. Thompson, "Qeeg and neurofeedback for assessment and effective intervention with attention deficit hyperactivity disorder (adhd)", *Introduction to Quantitative EEG and Neurofeedback: Advanced Theory and Applications, 2nd ed.. Edited by Budzynski TH. New York: AP*, vol. 502, pp. 337–364, 2009.

[131] L. L. Greenhill, "Pharmacologic treatment of attention deficit hyperactivity disorder.", *Psychiatric Clinics of North America*, 1992.

[132] B. S. Molina, S. P. Hinshaw, J. M. Swanson, L. E. Arnold, B. Vitiello, P. S. Jensen, J. N. Epstein, B. Hoza, L. Hechtman, H. B. Abikoff, *et al.*, "The mta at 8 years: Prospective follow-up of children treated for combined-type adhd in a multisite study", *Journal of the American Academy of Child & Adolescent Psychiatry*, vol. 48, no. 5, pp. 484–500, 2009.

[133] I. Buyck and J. R. Wiersema, "Resting electroencephalogram in attention deficit hyperactivity disorder: Developmental course and diagnostic value", *Psychiatry research*, vol. 216, no. 3, pp. 391–397, 2014.

[134] S. M. Snyder, H. Quintana, S. B. Sexson, P. Knott, A. Haque, and D. A. Reynolds, "Blinded, multi-center validation of eeg and rating scales in identifying adhd within a clinical sample", *Psychiatry research*, vol. 159, no. 3, pp. 346–358, 2008.

[135] S. M. Snyder, T. A. Rugino, M. Hornig, and M. A. Stein, "Integration of an eeg biomarker with a clinician's adhd evaluation", *Brain and behavior*, vol. 5, no. 4, 2015.

[136] J. F. Lubar, "Discourse on the development of eeg diagnostics and biofeedback for attention-deficit/hyperactivity disorders", *Biofeedback and Self-regulation*, vol. 16, no. 3, pp. 201–225, 1991.

[137] M. Arns, "Eeg-based personalized medicine in adhd: Individual alpha peak frequency as an endophenotype associated with nonresponse", *Journal of Neurotherapy*, vol. 16, no. 2, pp. 123–141, 2012.

[138] R. J. Barry, A. R. Clarke, and S. J. Johnstone, "A review of electrophysiology in attention-deficit/hyperactivity disorder: I. qualitative and quantitative electroencephalography", *Clinical neurophysiology*, vol. 114, no. 2, pp. 171–183, 2003.

[139] G. Ogrim, J. Kropotov, and K. Hestad, "The quantitative eeg theta beta ratio in attention deficit/hyperactivity disorder and normal controls: Sensitivity, specificity, and behavioral correlates", *Psychiatry research*, vol. 198, no. 3, pp. 482–488, 2012.

[140] M. A. Vollebregt, M. van Dongen-Boomsma, D. Slaats-Willemse, J. K. Buitelaar, and R. Oostenveld, "How the individual alpha peak frequency helps unravel the neurophysiologic underpinnings of behavioral functioning in children with attention-deficit/hyperactivity

disorder", *Clinical EEG and neuroscience*, vol. 46, no. 4, pp. 285–291, 2015.

[141] M. M. Lansbergen, M. Arns, M. van Dongen-Boomsma, D. Spronk, and J. K. Buitelaar, "The increase in theta/beta ratio on resting-state eeg in boys with attention-deficit/hyperactivity disorder is mediated by slow alpha peak frequency", *Progress in Neuro-Psychopharmacology and Biological Psychiatry*, vol. 35, no. 1, pp. 47–52, 2011.

[142] L. Chenxi, Y. Chen, Y. Li, J. Wang, and T. Liu, "Complexity analysis of brain activity in attention-deficit/hyperactivity disorder: A multiscale entropy analysis", *Brain research bulletin*, vol. 124, pp. 12–20, 2016.

[143] S. Khoshnoud, M. A. Nazari, and M. Shamsi, "Functional brain dynamic analysis of adhd and control children using nonlinear dynamical features of eeg signals", *Journal of integrative neuroscience*, no. Preprint, pp. 1–14, 2017.

[144] H. Zarafshan, A. Khaleghi, M. R. Mohammadi, M. Moeini, and N. Malmir, "Electroencephalogram complexity analysis in children with attention-deficit/hyperactivity disorder during a visual cognitive task", *Journal of clinical and experimental neuropsychology*, vol. 38, no. 3, pp. 361–369, 2016.

[145] H. Sohn, I. Kim, W. Lee, B. S. Peterson, H. Hong, J.-H. Chae, S. Hong, and J. Jeong, "Linear and non-linear eeg analysis of adolescents with attention-deficit/hyperactivity disorder during a cognitive task", *Clinical Neurophysiology*, vol. 121, no. 11, pp. 1863–1870, 2010.

[146] A. Ray, A RoyChowdhury, and S. Basak, "Effect of noise on generalized synchronization: An experimental perspective", *Journal of Computational and Nonlinear Dynamics*, vol. 8, no. 3, p. 031 003, 2013.